

Recent progresses in the chemistry of 12-membered pyridine-containing tetraazamacrocycles: From synthesis to catalysis.

Nicola Panza,^b Giorgio Tseberlidis,^c Alessandro Caselli,^{*b} and Rubén Vicente^{*a}

^a Departamento de Química Orgánica e Inorgánica, Instituto Universitario de Química Organometálica “Enrique Moles” and Centro de Innovación en Química Avanzada(ORFEO-CINQA), Universidad de Oviedo, Julián Clavería 8, 33006-Oviedo, Spain. Email: vicenteruben@uniovi.es

^b Department of Chemistry, Università degli Studi di Milano and CNR-SCITEC, Via Golgi, 19, 20133 Milano, Italy. Email:

^c Department of Materials Science and Solar Energy Research Center (MIB-SOLAR), University of Milano-Bicocca, Via Cozzi 55, I-20125 Milano, Italy.

Abstract

This article provides an overview (non-comprehensive) on recent developments regarding pyridine-containing 12-membered tetraazamacrocycles with pyclen or Py₂N₂ backbones and their metal complexes from 2017 to the present. Firstly, the synthesis of newly described ligands and complexes with relevance to medicine are described. The second part deals with the reactivity of complexes bearing these ligands and their uses in catalysis. Special emphasis on the role of the pyridine-containing ligand is highlighted along the text.

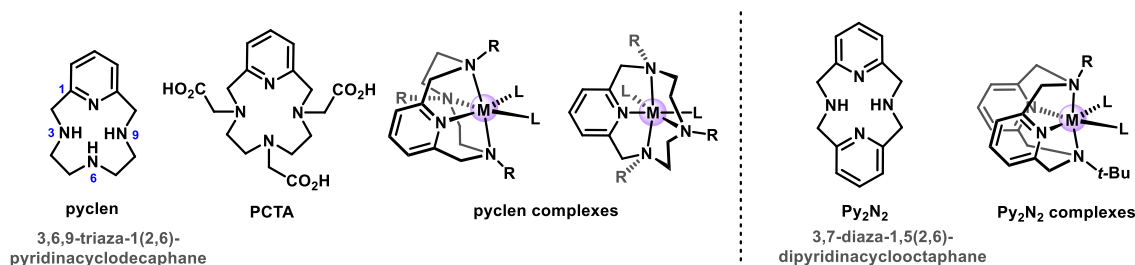
1. Introduction.

Macrocyclic structures containing nitrogen atoms are widespread in nature. Indeed, polyazamacrocycles play fundamental role in biological processes as illustrated when considering porphyrins or related compounds.^{1,2} These compounds are an everlasting source of inspiration and the desire of mimicking them has been always an aspiration for chemists. The study of polyazamacrocycles involves joint research from both organic synthetic and inorganic or organometallic chemists but, importantly, the utility of these ligands falls far beyond chemistry. For instance, polyazamacrocycles and their complexes have been extensively used in catalysis but have found an irreplaceable place in the field of medicine as therapeutic or diagnosis agents,³ as well as biological sensors. In this sense, the approval of gadolinium(III) complex Magnevist[®], showing an *acyclic* polyazadentate ligand for magnetic resonance imaging (MRI) contrast agent (CA) by FDA in 1988 was a landmark. Since then, 11 more MRI CA based on gadolinium(III) complexes have been approved,^{4,5} including some with *cyclic* polyazamacrocyclic ligands. Due to relative toxicity and cost of gadolinium complexes, extensive search to develop less toxic, more stable MRI CA which operates at lower doses has been accomplished.⁶

With virtually countless imaginable possibilities, there are several polyazamacrocyclic architectures that are commonly employed. Among them, tetraaza-12-membered macrocycles, in which at least one of the *N*-atoms belongs to a pyridine ring, have received particular

attention. In fact, gadopiclesol, a gadolinium(III) complex coordinated to a pyridine-containing polyazamacrocyclic ligand has been recently evaluated in Phase III clinical trials as MRI CA with positive results, as reported by Geubert. This fact could be attributed to the particular properties conferred to the macrocyclic ligand by the presence of the pyridine(s) ring(s) which are, subsequently transferred to the complex when coordinated. Thus, the kinetic stability is strongly affected by the presence of a pyridine into the polyazamacrocyclic skeleton by increasing the conformational rigidity and tuning the basicity. These features are of paramount importance when considering these complexes for MRI CA and for other applications. In spite of this stability, complexes from pyridine-containing macrocycles exhibit a remarkable reactivity. Indeed, the deviation from planarity of the donor atoms imposed by the pyridine influences the metal complexes in two related ways. On the one hand, the small cavity of the 12-membered macrocyclic ligand forces a coordination geometry which facilitates the approach of the reagents in *cis* position. On the other hand, the geometry and electronic properties enable access to uncommon high oxidation states of the coordinated metal atom. These features have been applied to the study of fundamental stoichiometric organometallic reactions as well as in catalysis.

Although several type of ligands could meet the structural description, this Perspective article deals with two specific skeletons, which are the most frequently employed and studied (Scheme 1). With one single pyridine ring, 3,6,9-triaza-1(2,6)-pyridinacyclodecaphane is the most commonly found structure of tetraaza-12-membered macrocycles containing a single pyridine ring. Several abbreviations have been utilized to name easily this compound, but in the recent times the *alias* **pyclen** seems to have imposed. A pyclen derivative, **PCTA**, is also well-known by this term. Herein, both ligands will be designated in this manner in the text and schemes. Regarding the presence of two pyridine rings, symmetric 3,7-diaza-1,5(2,6)-dipyridinacyclooctaphane is the most typical ligand. In general, this ligand is simply abbreviated by **Py₂N₂**, which again will be used herein for this specific ligand. Normally, authors tend to add more information about the ligand on the abbreviations. While this might be suitable for a research paper, it turns unmanageable for a revision and, therefore, only easily recognizable ligands will be designated with common names. The rest of them will be named **Ln** with consecutive numbers. With respect to the metal complexes, the drawings in Scheme 1 will be used, although many possibilities for the 3D description exists. Metal complexes will be designated as **M(m)L_n** (m = formal oxidation state; n = ligand number) along text and schemes, regardless the rest of inner and outer sphere ligands, and the later will be only included when necessary.



Scheme 1. Structure of the pyridine-containing tetraaza-12-membered macrocycles disclosed.

A recent review focused on catalytic applications involving this type of ligands from some of the authors covered relevant literature up to 2016.⁷ However, the increasing number

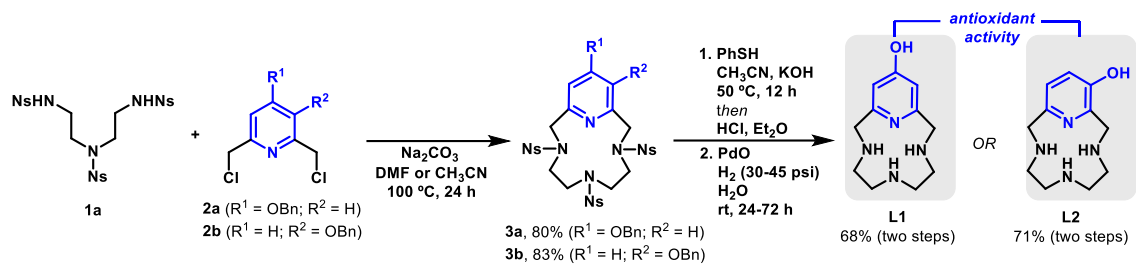
of works dealing with these ligands and its relevance justifies the need to cover, although in a relatively brief manner, the progress done in the last years, including works reported already in 2022. Two well-differentiated parts comprises this work. The first one is devoted to the synthesis of 12-membered-pyridine containing macrocycles and some of their complexes in works mainly oriented to the development of MRI CA or related applications. Describing properties relevant to medical applications are beyond the scope of this article and will only be indicated briefly in selected examples. The second part is focused on the reactivity of metal complexes containing this class of ligands starting with redox processes, especially biomimetic reactions, and continues with studies on C–C bond formation reactions. Several aspects such as complex synthesis, stoichiometric chemistry and their role as catalysts are discussed with a focus on the influence of the pyridine ring.

2. Synthesis of pyridine-containing 12-membered tetraazamacrocycles and their complexes for medicinal uses.

2.1. PycLEN ligands.

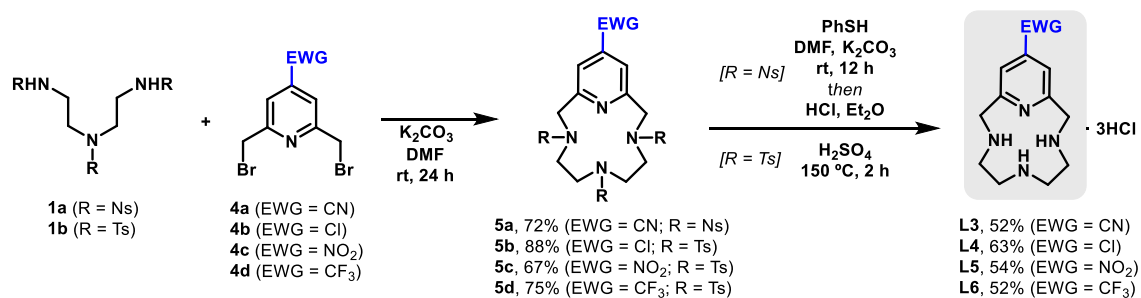
The synthetic strategy to prepare pycLEN-type compounds still relies in the Richman-Atkins procedure described in 1974.⁸ This straightforward approach makes use of a given 2,6-difunctionalized pyridine and a protected triamine. The two fragments can be assembled under certain reactions conditions and, in general, with good yields regardless the unfavourable entropic factor. Indeed, Richman-Atkins procedure constitutes a quite robust synthetic method, especially for structurally simple pycLEN type ligands. The main issue of the approach resides on retarding and tedious protection-deprotection steps. This fact becomes apparent when introducing additional substituents. Normally, longer synthetic sequences are unavoidable in those cases. Moreover, the introduction of different groups at each *N* atom of the macrocycle, requires the preparation of specifically substituted triamines as starting materials. In the recent years, the catalogue of new pycLEN related macrocycles has been fruitfully expanded.

The group of K. C. Green has been actively working in the preparation of new pycLEN derivatives with different purposes. For instance, apart from MRI CA uses, Green's group found in 2013 that simple **pycLEN** had promising properties as antioxidant in a biological context.⁹ In particular, the distinctive structure of **pycLEN** provided two ways to control oxidation processes which might eventually induce cell death. On the one hand, the pyridine ligand showed antioxidant properties. On the other hand, the macrocyclic backbone served as a chelating agent for copper, hindering Cu(II)-induced redox oxidative stress processes on cells. This discovery triggered new studies on the ability of pycLEN ligands as antioxidants with special focus on the effect of substituents at position 4 in the pyridine ring in the pycLEN ligand (Scheme 2). This strategy is based on the reasonable assumption that this modification might influence the antioxidant activity without compromising the chelation ability. Thus, Green and co-workers described the synthesis of hydroxyl-substituted pycLEN-OH macrocycles **L1** and **L2**, through a typical Richman-Atkins macrocyclization of benzyloxy-protected pyridine derivatives **2a-b** with nosyl-protected triamine **1** and subsequent removal of all protecting groups. As expected, the presence of the hydroxyl moiety significantly enhanced the antioxidant activity. Moreover, their chelation abilities were demonstrated with the preparation of several ions from transition,^{10,11,12} and group 2 metals.¹³



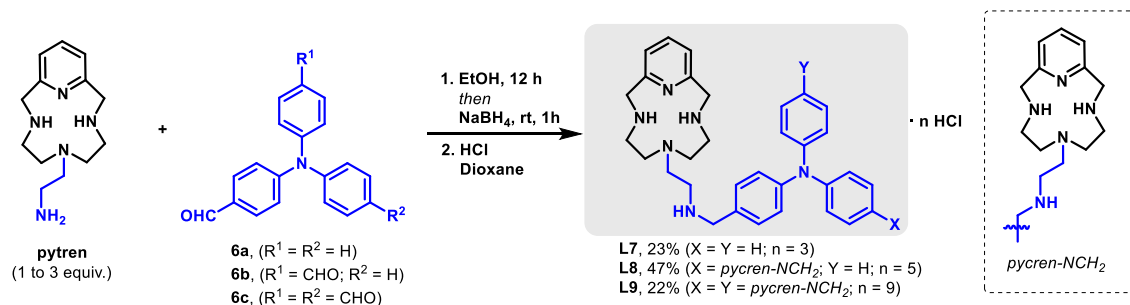
Scheme 2. Synthesis of OH-substituted pycen ligands **L1** and **L2**.

A related contribution from Green's group focused on providing methodology for the synthesis of pycen macrocycles bearing electron-withdrawing groups at position 4 on the pyridine ring (Scheme 3).^{14,12} Conventional methodologies were employed to prepare the required 4-substituted *bis*-(2,6-bromomethyl)pyridine derivatives **4a-d**, whose better solubility with respect to chloro analogues ensured a more efficient cyclization. Moreover, the selection of the protected triamines **1** relied on the functional group compatibility for the deprotection step. With these considerations, macrocyclization under Richman-Atkins conditions led to the formation of the macrocycles **5a-d** in good yields and the subsequent removal of the protecting groups allowed an efficient synthesis of pycen derivatives **L3-L6**.



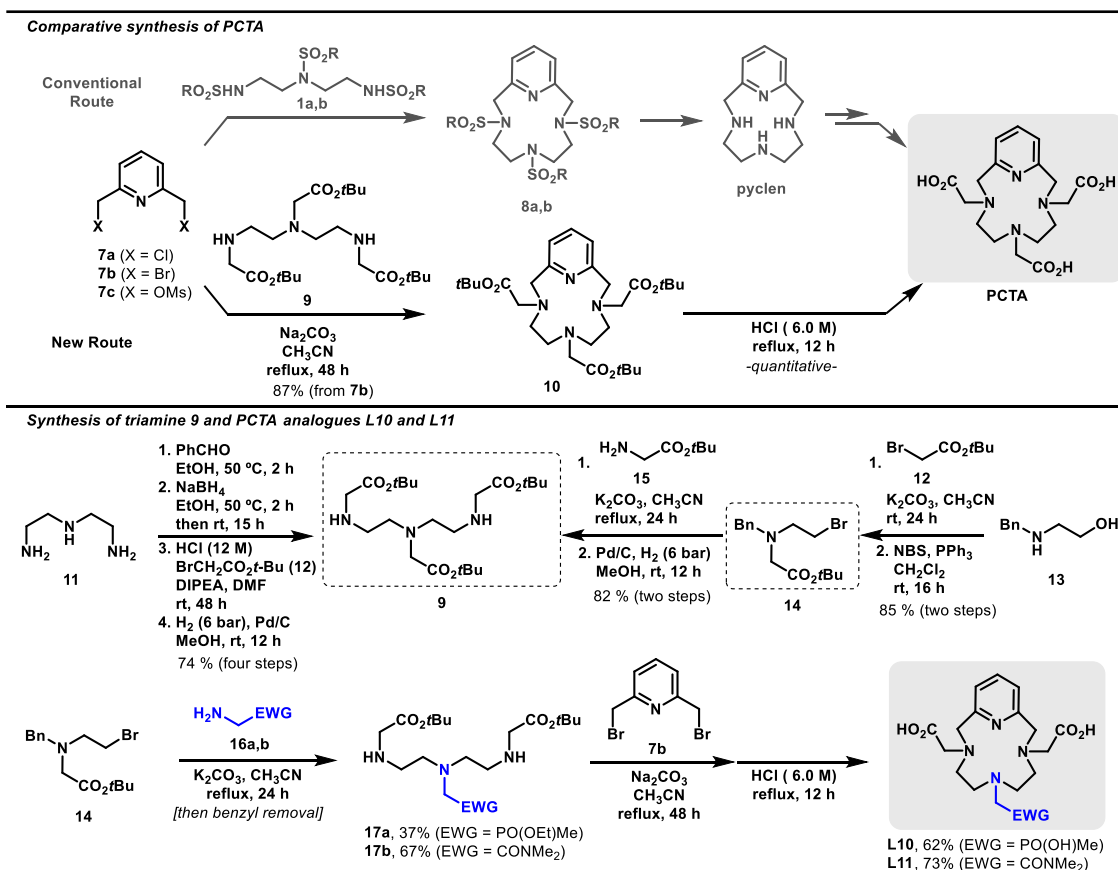
Scheme 3. Synthesis of pycen ligands **L3-L6** with electron-withdrawing groups at pyridine ring.

González-García, Villar, García-España and co-workers reported the synthesis of pycen derivatives **L7-L9** decorated with triphenylamine, as hydrochloride salts (Scheme 4).¹⁵ These ligands were prepared by using the required amount of known *pytren* macrocycle¹⁶ and triarylamines derivatives **6** via condensation, reduction and precipitation with HCl. These triphenylamine derivatives of pycen **L7-L9** strongly bind some G-quadruplex (G4s), non-canonical DNA secondary structures, without disturbing their structure. Due to the relevant roles attributed to G4s in biological processes, this study showed the potential of these ligands in therapeutic uses.



Scheme 4. Synthesis of triphenylamine-derived pyclen ligands L7-L9.

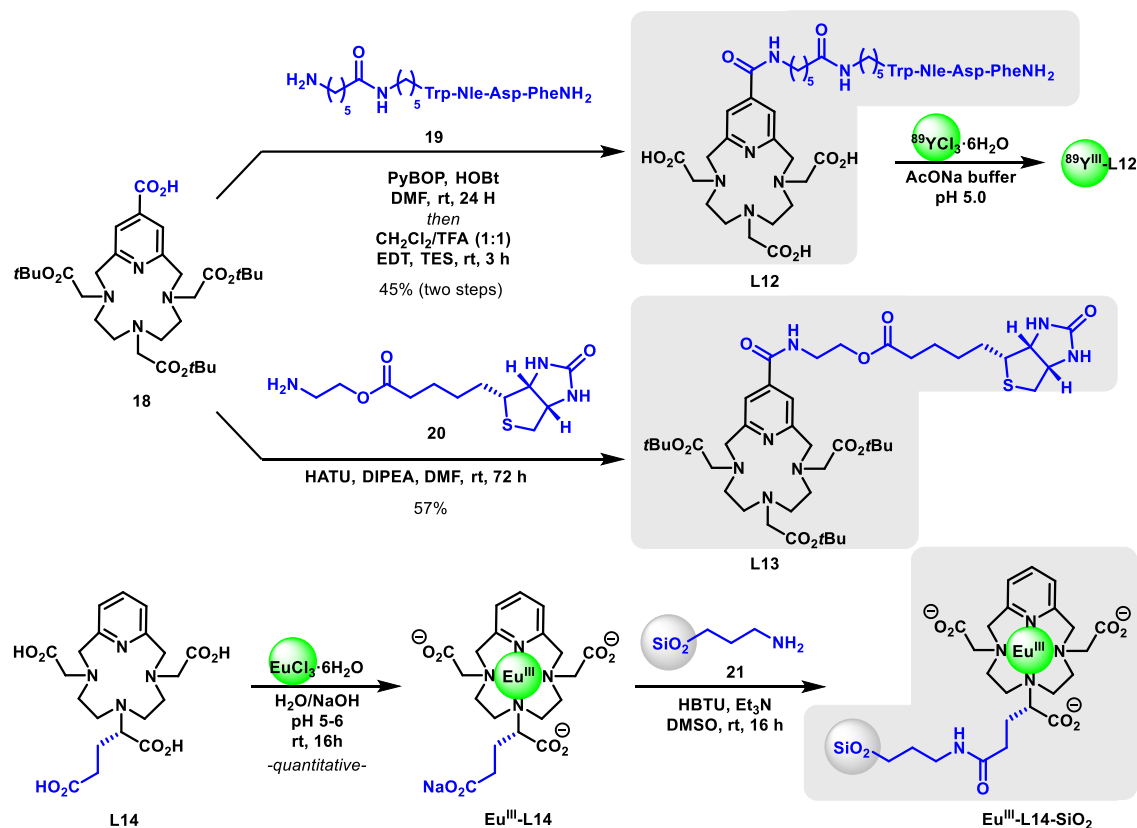
Typically, the synthesis of **PCTA** requires the preparation of **pycLen**. Thus a relatively long sequence starts with a macrocyclization using sulfonyl-protected triamines **1** and 2,6-disubstituted pyridines **7**.¹⁷ Apparently straightforward tosyl removal to afford **pycLen** and subsequent alkylation reactions are then accomplished, yet they are tricky steps that proceed in modest yields. In 2018, Galaup, Picard and co-workers reported an alternative method for the synthesis of **PCTA** and analogues,¹⁸ by using previously reported triamine **9** (Scheme 5).¹⁹ Amine **9** undergoes macrocyclization in similar efficiency when compared with the traditional method, but allows a quantitative transformation to **PCTA**. Although the key triamine **9** could be prepared from the unprotected amine **11**, an alternative approach from commercially available amine **13** was also reported. Importantly, using common synthetic intermediate **14**, this route allowed the preparation of **PCTA** analogues **L10** and **L11** bearing an amide or a phosphinate coordinating groups tethered at position 6 of the macrocycle. Interestingly, **L10** and **L11** were used to prepare complexes from Eu(III), Tb(III) and Gd(III).



Scheme 5. New synthesis of **PCTA** and **L10-L11** analogues from suitable triamines.

Subsequently, Leygue, Picard and co-workers reported the preparation of bifunctional chelators based on the **PCTA** macrocycle core, which could be suitable ligands for bioconjugation (Scheme 6).²⁰ Based on the synthetic approach described before by Picard,¹⁸ they reported the synthesis of ligands **L12** and **L13** decorated with additional carboxylic acid groups at position 4 of the pyridine or tethered at position 6 of the macrocycle, respectively. The presence of these

functionalities was exploited to prepare representative conjugates. For instance, cholecystokinin peptide derivative **19** and biotin derivative **20** were coupled with macrocycle **18** to afford the corresponding conjugates **L12** and **L13**, respectively. Importantly, Y(III) complex $^{89}\text{Y}^{\text{III}}\text{-L12}$ could be prepared without interference of the peptide substituent. Moreover, quantitative coordination of compound **L14** to Eu(III) formed the corresponding complex $\text{Eu}^{\text{III}}\text{-L14}$ showing an additional carboxylate moiety. This remote group served for the immobilization using 3-aminopropyl SiO_2 (**21**) as solid support.

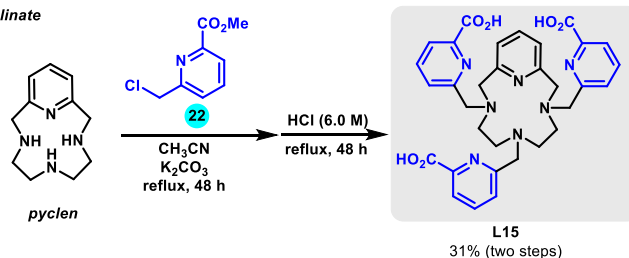


Scheme 6. Synthesis of bifunctional ligands **L12-L14** for bioconjugation and immobilization.

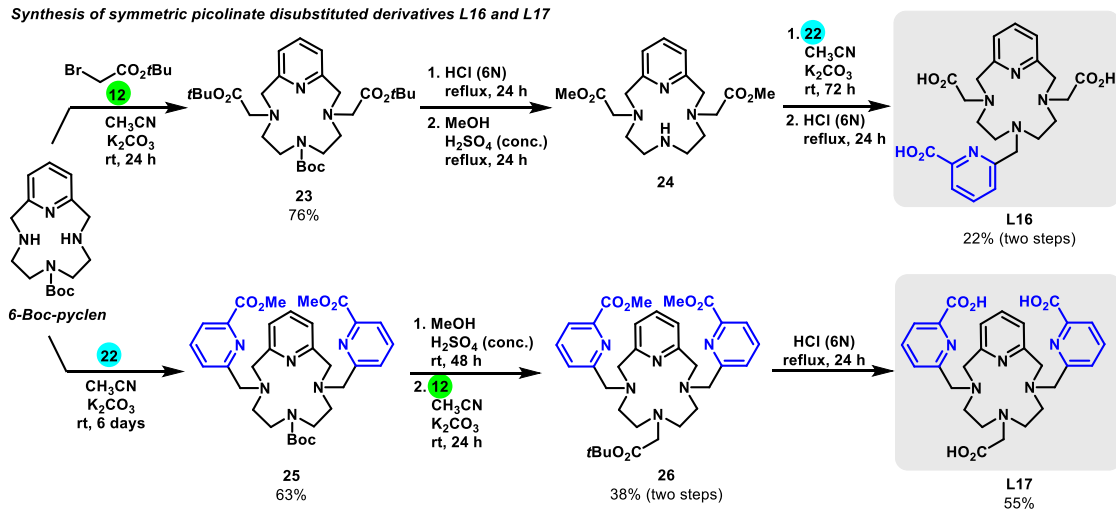
Among the possibilities to modulate pyclen properties by introducing substituents, modifications on well-studied **PCTA**,¹⁷ constitutes one of the preferred choices. For instance, the replacement of carboxylate moieties by 2-picolinates has been employed to generate the family of picolinate pyclen ligand derivatives **L15-L19** expanding the number of coordination sites (Scheme 7). Indeed, the synthesis of all possible carboxylate/picolinate replacements was patented by Tripier, Rousseaux and co-workers,²¹ and further discussed afterwards in a series of reports.^{22,23,24} The easiest synthesizable compound was symmetric **L15** ligand. Indeed, it was directly prepared by alkylation of **pyclen** with picolinate methyl ester **22** and subsequent hydrolysis in a decent 31% overall yield. Other symmetric ligands **L16** and **L17** could also be prepared in a straightforward manner from easily available **6-Boc-pyclen**. Here, the key of the strategy resides in the sequence of alkylation events highlighted in the scheme with coloured numbers for the alkylating agents. This programmable approach allowed the synthesis of both ligands in reasonable yields and with complete positional selectivity for the introduction of the picolinic acid substituents. In contrast, non-symmetrical structures of **L18** and **L19** ligands imposed a more elaborated synthetic route. The success on the synthesis relied on the use of

pyclen oxalate **28**, which can be directly prepared by treatment of *pyclen* with diethyl oxalate (**27**). From common intermediate **28**, the use of same alkylating reagents following an adequate sequence along with the required functional groups manipulations, led to the preparation of both ligands in useful yields. A variety of picolinate-substituted metal complexes and their properties have been reported. For instance, stable complexes of $^{90}\text{Y}^{3+}$ for radiolabelling applications have been prepared.^{22,23} Other complexes from lanthanide ions such as Gd(III), Eu(III), Tb(III), Lu(III) or Yb(III) showed promising properties as luminescent probes or radiopharmaceuticals.^{25,26}

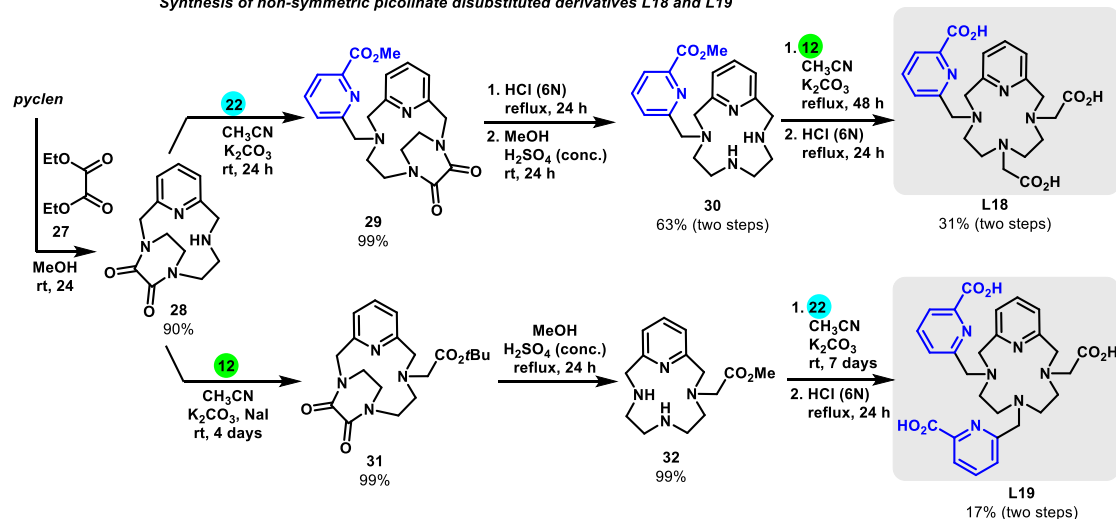
Synthesis of symmetric picolinate trisubstituted derivative L15



Synthesis of symmetric picolinate disubstituted derivatives L16 and L17



Synthesis of non-symmetric picolinate disubstituted derivatives L18 and L19



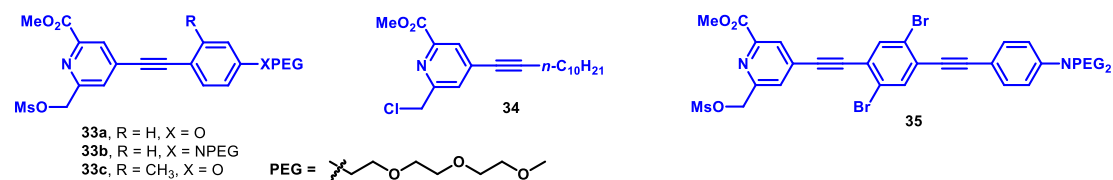
Scheme 7. Synthesis of picolinate-substituted pyclen ligands.

According to the potential demonstrated by metal complexes with picolinate-decorated ligands **L15-L19**, further modifications were introduced for a refined tuning of their properties and to facilitate their applicability in medicinal chemistry. Thus, the introduction of donor- π -conjugated-acceptor “*antennas*” and the subsequent preparation of the metal complexes was recently accomplished (Scheme 8). For instance, ligands **L20-L22** with pending *antennas* at picolinate positions 3 and 6 were prepared from monomethyl ester pyclen derivative **32**. An initial alkylation with prefunctionalized mesylated pyridines **33a-c** led to the corresponding triester derivatives **36a-c** in modest yields, due to the difficulties found for their purification.^{27,28} After saponification, a set of lanthanide complexes were prepared in reasonable yields. Some of these complexes exhibited promising properties as 1- or 2-photon luminescence bio-probes. Importantly, preliminary studies highlighted the absence of significant toxicities in small animal models.

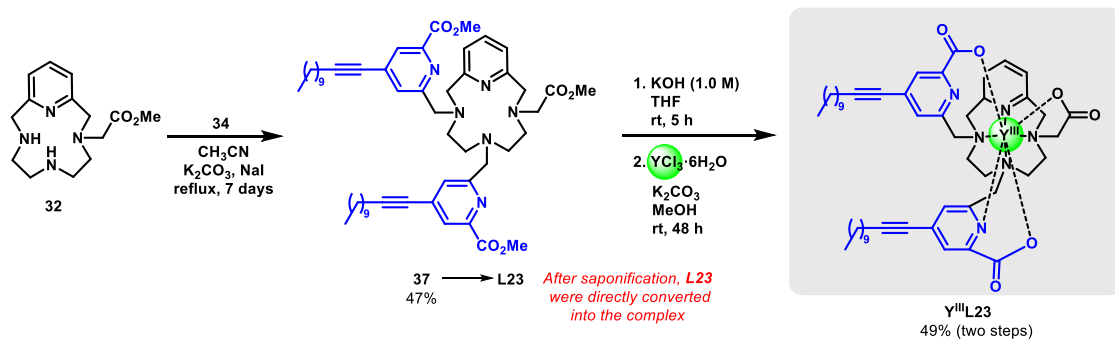
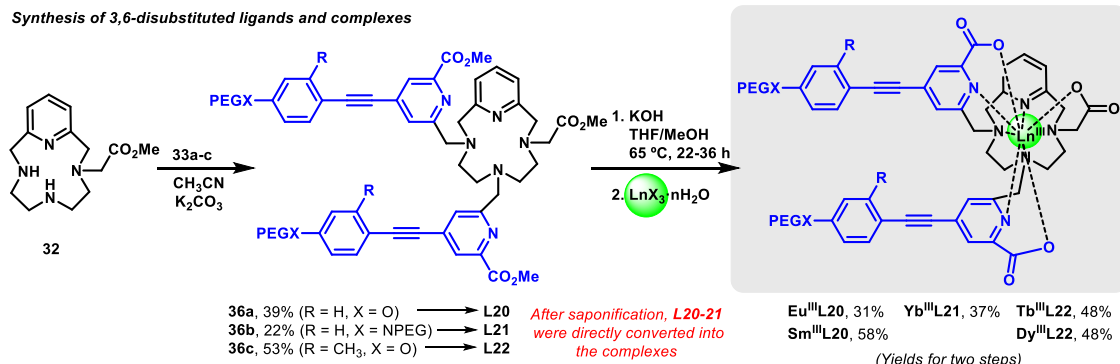
With the aim to modulate the lipophilic nature of this type of ligands and complexes, the introduced *antenna* was decorated with a long alkyl chain using mesylated picolinate derivative **34**. Following the same synthetic sequence, ⁹⁰Y(III) complex **Y^{III}L23** was prepared.²⁹ The presence of the saturated alkyl chain did not affect the radiolabelling efficiency of **Y^{III}L23**. Moreover, the increased lipophilicity allowed for an easier extraction of the complex.

The introduction of two picolinate *antennas* in positions 3 and 9 was also reported.²⁸ In an analogous synthetic sequence, pyclen derivative **38** and mesylated picolinate **33a** were employed for the synthesis of Eu(III) complex **Eu^{III}L24**. Nevertheless, properties of this symmetrically substituted complex were less encouraging.

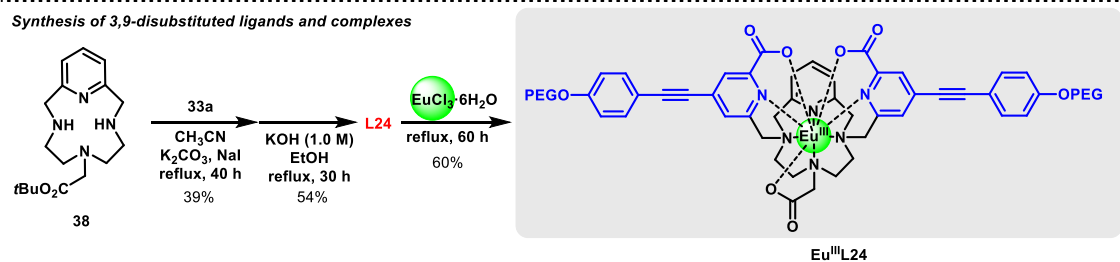
Besides, Gd(III) complex **Gd^{III}L25** bearing a single picolinate *antenna* at position 3 was also described.³⁰ The synthesis required the use of disubstituted pyclen ligand **39** and more elaborated picolinate **35**. Following the same synthetic approach, complex **Gd^{III}L25** was obtained in a remarkable high overall yield. Potential applications as a theranostic agent were reported for this complex.



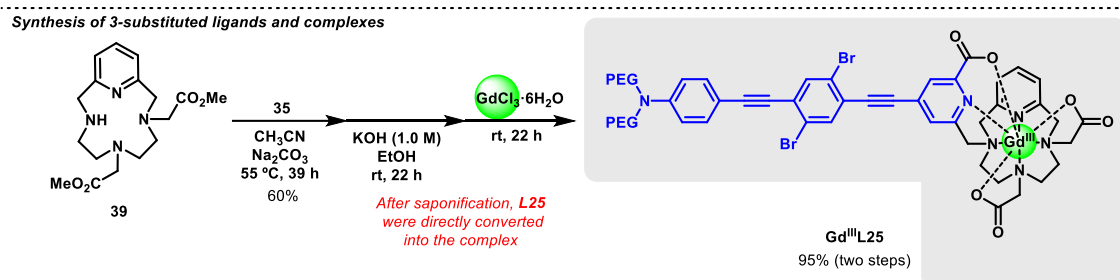
Synthesis of 3,6-disubstituted ligands and complexes



Synthesis of 3,9-disubstituted ligands and complexes



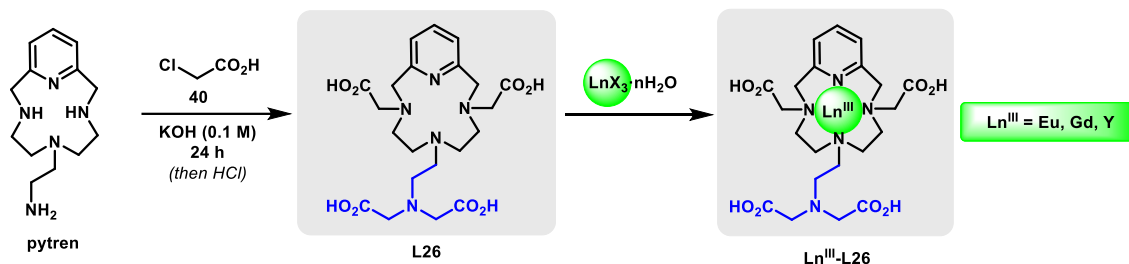
Synthesis of 3-substituted ligands and complexes



Scheme 8. Introduction of conjugated *antennas* in picolinate-substituted ligands and complexes.

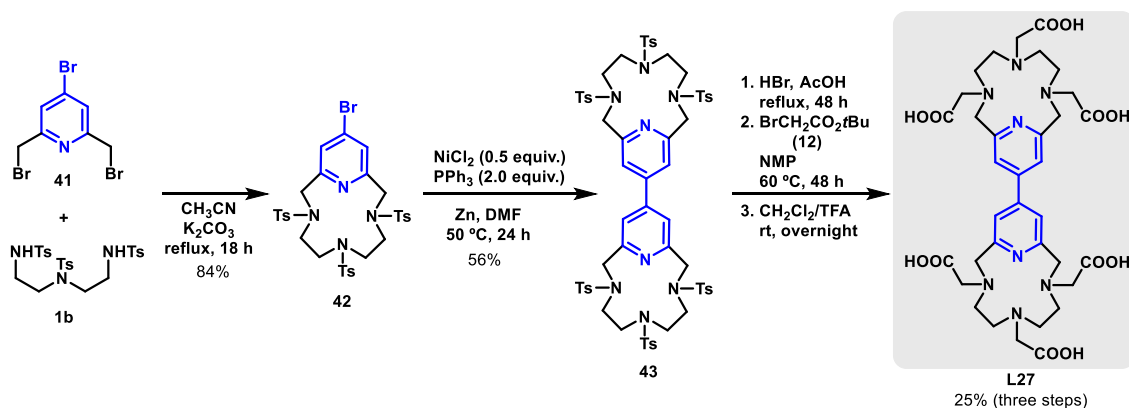
Platas-Iglesias, Albelda and co-workers reported the synthesis of the new PCTA derivative macrocyclic ligand **L26** showing a scorpion-like structure (Scheme 9).³¹ Preparation of **L26** was accomplished by extensive alkylation with chloroacetic acid (**40**) using previously described **pytren** macrocycle.¹⁶ Then, some lanthanide complexes with Eu(III), Gd(III) and Y(III) complexes Ln^{III}**L26** were prepared. It should be noticed that yield for the synthesis of ligand **L26**

was not given and the procedure for the preparation of the complexes was not thoroughly described. Remarkably, Eu(III) and Y(III) complexes formed aggregates in solution at high pH values, a phenomenon that has been rarely observed in lanthanide-pyclen based complexes.



Scheme 9. Synthesis of scorpionand ligand **L26** and lanthanide complexes.

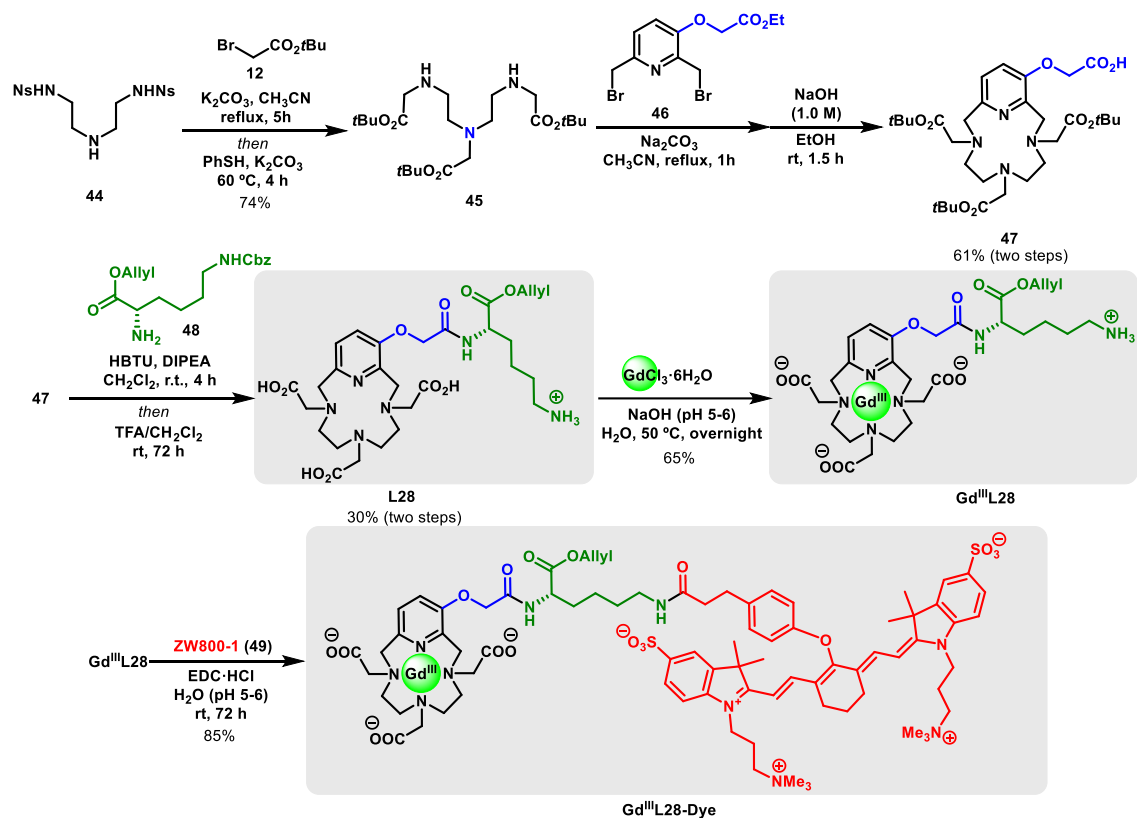
Botta, Tei and co-workers recently reported the synthesis of binuclear Gd(III) complexes.³² In particular, the synthesis of PCTA dimer **L27** ligand bearing a 4,4'-bipyridine backbone was reported (Scheme 10). The synthesis relied on the use of 4-bromo-2,6-bis-(bromomethyl)-pyridine (**41**) and tosyl-protected triamine **1b** to assemble the macrocycle **42**, via Richman-Atkins reaction. Ni-catalysed homocoupling reaction led to bipyridine derivative **43**. Subsequent removal of tosyl group, alkylation and ester hydrolysis led to ligand **L27**. The binuclear Gd(III) complex was generated by mixing **L27** and two equivalents GdCl₃ at pH 6.0. Interestingly, this binuclear complex showed a three-times higher relaxivity values than some commercial contrast agents, a feature relevant to a potential clinical application since it should allow lowering the dose required.



Scheme 10. Synthesis of **L27** with a 4,4'-bipyridine backbone.

The preparation of monstrous PCTA derivative **L28** ligand as bimodal probe for MRI and photoacoustic imaging was reported by Laurent and co-workers (Scheme 11).³³ The ligand comprised three distinguishable parts, pyclen, aminoacidic linker and an organic dye. The pyclen fragment required the use of triamine **45**, obtained in one-pot from di-nosyl amine **44**. Richman-Atkins cyclization with 3-substituted pyridine **46** afforded the macrocycle, which after chemoselective saponification led to ligand **47** showing the suitable functionalization to connect all fragments. HBTU-promoted amide formation of **47** with the lysine residue of aminoacid derivative **48** joined the first two fragments to afford **L28** after complete hydrolysis. Notably, the yield was remarkable when considering the functionalization. Formation of Gd(III) complex

Gd^{III}L28 took place in decent yield without interference of the aminoacid residue. The last step was the introduction of the fluorophore ZW800-1 (**49**), which was accomplished using EDC under pH control to avoid metal dissociation, affording compound **Gd^{III}L28-Dye**. Satisfyingly, the design proved valid as compound **Gd^{III}L28-Dye** was efficient in both medical probes and open a promising door for this type of compounds in medicine.

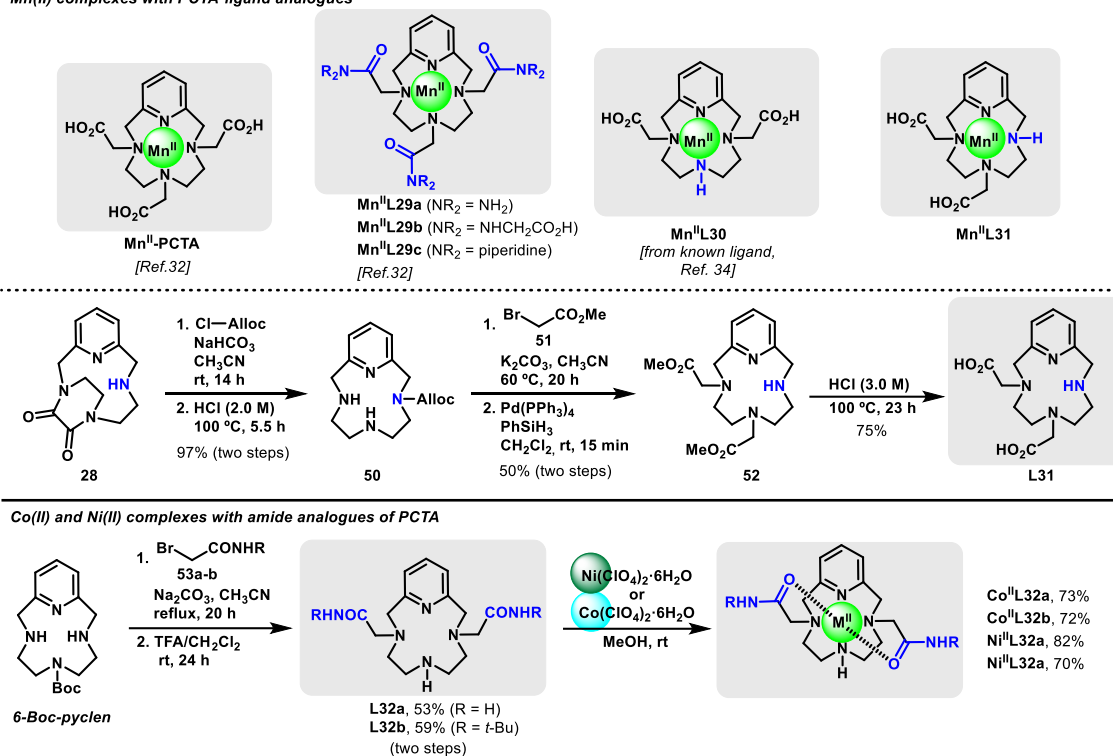


Scheme 11. Synthesis of **Gd^{III}L28-Dye** as MRI and photoacoustic imaging bimodal probe.

In the recent years, in-depth studies have been accomplished to develop Mn(II)-based complexes as *in vivo* MRI CA in order to replace more expensive and toxic Gd(III) complexes. Among the plethora of chelating ligands available, 12-membered pyridine-containing tetraazamacrocycles have shown promising properties.³⁴ This fact has triggered the search for new ligands based on slight modifications of **pyclen** and **PCTA** basic frameworks.

Mn^{II}-PCTA complex and analogues bearing amide groups were reported in 2018,³⁴ but other versions based on ligands lacking of one of the acetate arms were later reported (Scheme 12).³⁵ While 3,9-diacetate substituted ligand **L30** was already known,³⁶ the 3,6 substitution pattern shown in ligand **L31** required an elaborated synthesis. Thus, the synthesis started with 3,6-diprotected pyclen oxalate **28**, whose N–H-free atom was protected with the Alloc group to improve its solubility. Then, liberation of 3 and 6 positions, alkylation, Alloc removal and hydrolysis led to 3,6-diacetate-9-N–H-free ligand **L31**. In a similar context, Platas-Iglesias, Valencia and co-workers described the synthesis of 3,6- and 3,9-diacetamide-9-N–H free ligands **L32a-b**, and the corresponding Co(II) and Ni(II) complexes were prepared.³⁷ These complexes probed their ability, even though modest, to serve in chemical exchange saturation transfer (CEST), an emerging NMR sequence to generate images and contrast.

Mn(II) complexes with PCTA ligand analogues



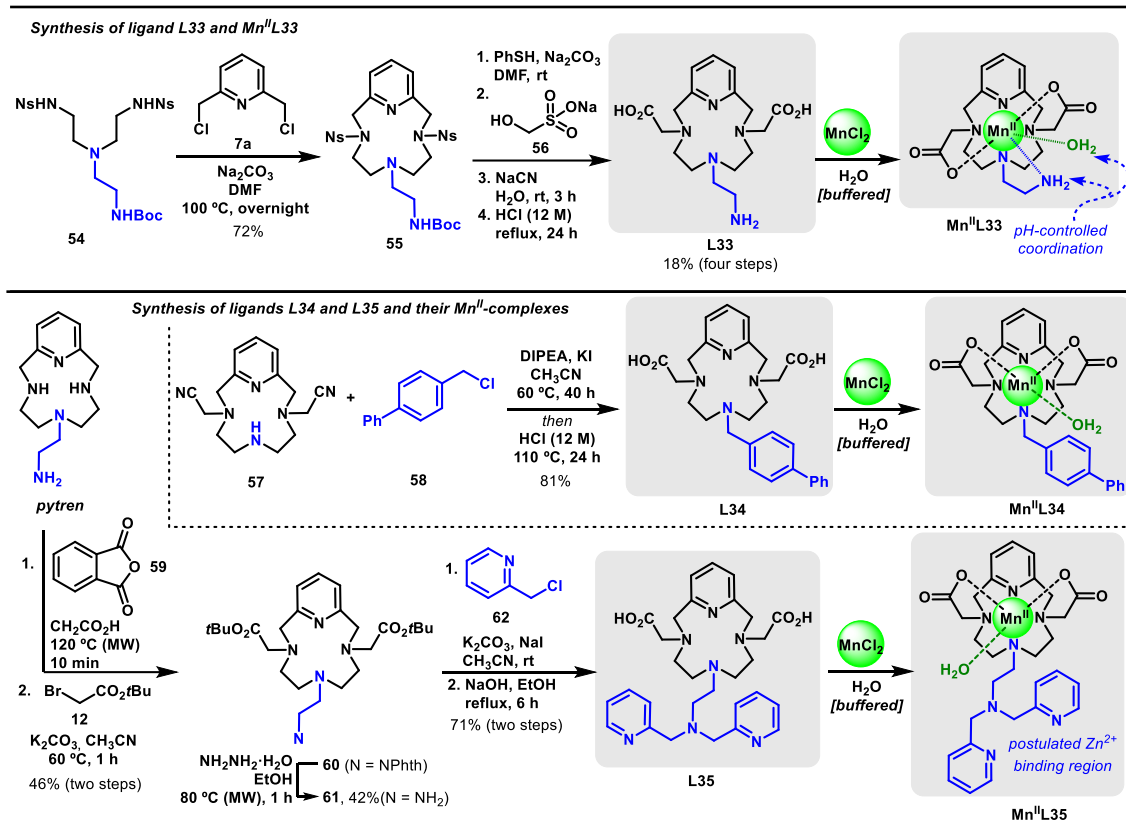
Scheme 12. PCTA-derived ligands **L29-L32** and their Mn(II) complexes as potential MRI CA.

More elaborated structures have been prepared in the search for ideal MRI CA candidates. For instance, Tircsó and co-workers reported the synthesis of PCTA analogue ligand **L33**, in which the acetate residue at position 6 of the macrocycle was replaced by 2-ethylamine moiety (Scheme 13).³⁸ This apparently innocuous modification required a remarkable synthetic effort. Indeed, orthogonally-protected tetraamine **54**³⁹ was employed for the macrocyclization with suitable pyridine **7a**. The introduction of the acetate moieties at positions 3 and 9 was performed by nosyl deprotection, two-step alkylation with sodium formaldehyde bisulfite (**56**) and subsequent addition of NaCN. Hydrolysis of cyano groups to the acid with a concomitant Boc-group removal led to ligand **L33**. The corresponding Mn(II) complex **Mn^{II}L33** formed showed good properties as CA candidate. Interestingly, the response of the complex was pH-dependent, opening access to its use as pH-responsive agent.

The synthesis of other ligands and Mn(II)-complexes bearing amine substituents at position 6 of the macrocycle was also disclosed by Tircsó and co-workers. For instance, ligand **L34** bearing biphenyl backbone was prepared by alkylation of 3,9-acetonitrile-disubstituted pyclen precursor **57**³⁶ with commercially available 4-chloromethyl-1,1'-biphenyl (**58**) followed by hydrolysis.⁴⁰ Various complexes from 3rd row metals were prepared and the Mn(II)-complex **Mn^{II}L34** showed enhanced stability due to the presence of biphenyl group allowing the reduction of the dose required for MRI.

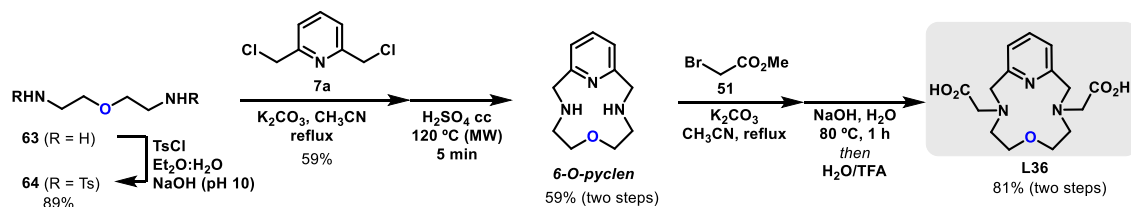
More recently, Tircsó's group reported the synthesis of a new ligand **L35** decorated with a tridentate arm at position 6 of the macrocycle.⁴¹ A relatively long synthetic sequence was required in this case. Thus, primary amine of *pytren* was protected as phthalimide to facilitate introduction of *tert*-butyl acetate groups by the alkylation. Subsequent deprotection of the amine and its dialkylation with 2-chloromethylpyridine (**62**) and ester hydrolysis led to ligand

L35 in a decent overall yield. In this case, the prepared Mn(II)-complex **Mn^{II}L35** showed inertness towards Zn(II) ions pointing out to the feasibility to use **Mn^{II}L35** as zinc responsive MRI CA candidate.



Scheme 13. 6-Substituted PCTA-derived ligands **L33-L35** and their Mn(II) complexes.

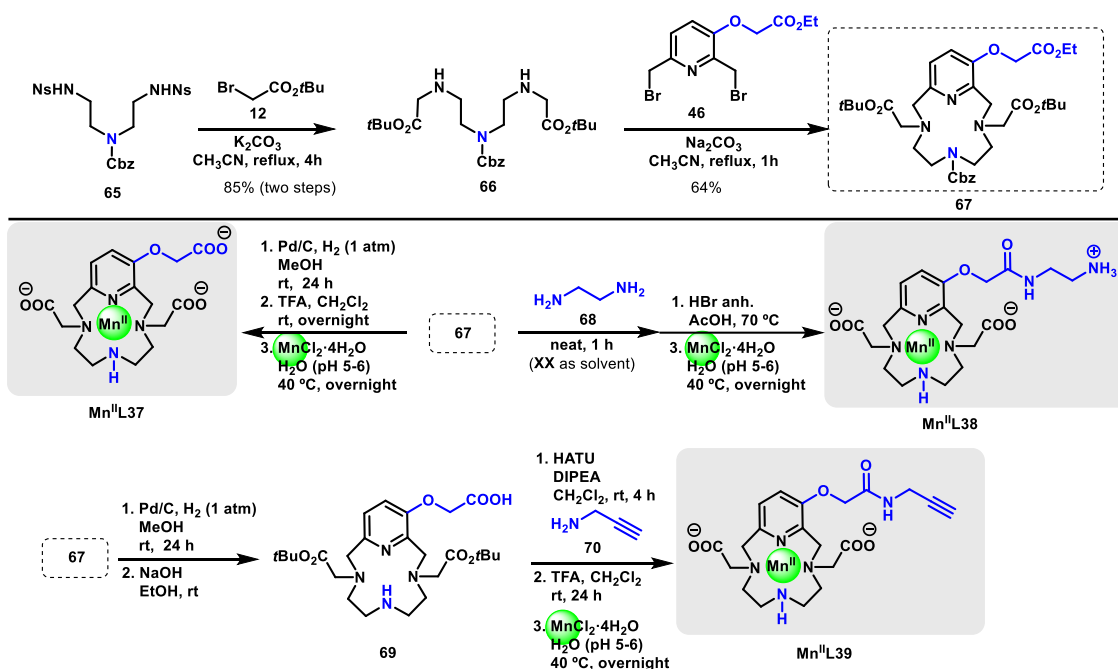
Further modifications on pyclen core were performed to expand the scope of ligands supply for Mn(II) complexes. In this context, the preparation of oxygen-substituted pyclen-like macrocycle **6-O-pyclen**, whose core structure differs from pyclen by a single atom, was tackled by Tircso's group (Scheme 14).⁴² Using previously described *bis*(2-aminoethyl)ether (**63**),⁴³ tosyl protection and Richman-Atkins macrocyclization with pyridine derivative **7a** allowed the assembly of the core ligand in good yield. Subsequently, the direct deprotection afforded **6-O-pyclen** in moderate yield. Finally, alkylation with **51**, saponification and protonation were accomplished to prepare **L36**, allowing the synthesis of the Mn(II) complex, among others.



Scheme 14. Synthesis of **6-O-pyclen** ligands.

Finally, a set of Mn(II) complexes bearing ligands functionalized at position 3 of the pyridine ring and N-H-free group at position 6 of the macrocycle were prepared by Laurent and

co-workers (Scheme 15).⁴⁴ The synthesis of these ligands relied on a previous work from the same group,³³ making use of orthogonally protected triamine **65**.⁴⁵ Alkylation of **65** with **66**, followed by Richman-Atkins cyclization with 2,3,6-trisubstituted pyridine **46** led to macrocycle **67** as unique precursor for further manipulations at position 3 of the pyridine. Thus, Cbz deprotection, hydrolysis and complexation led to $\text{Mn}^{\text{II}}\text{L37}$. Alternatively, amine formation by treatment of **67** with ethylenediamine (**68**), extensive hydrolysis and treatment with MnCl_2 , enabled the synthesis of $\text{Mn}^{\text{II}}\text{L38}$. This complex is also a potential pH responsive MRI CA. Finally, a sequence comprising Cbz deprotection and chemoselective saponification afforded macrocycle **69**. In this manner, HATU-promoted amide formation with propargylamine (**70**) and ester hydrolysis set the stage for the formation of $\text{Mn}^{\text{II}}\text{L39}$. The presence of the alkyne group might eventually facilitate the bioconjugation of the complex.



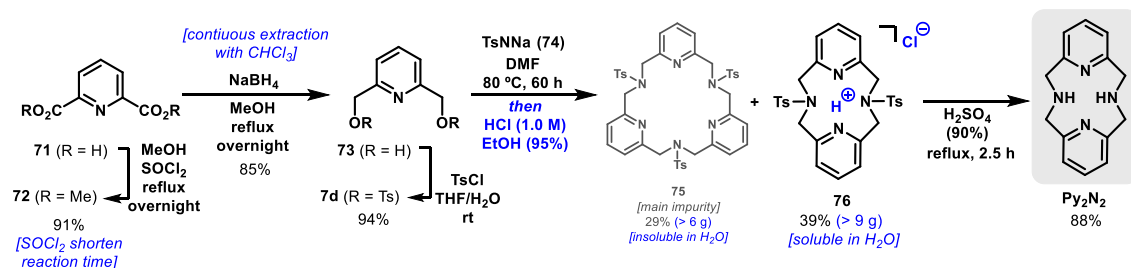
Scheme 15. Synthesis of $\text{Mn}^{\text{II}}\text{L37-39}$ with pyclen ligands substituted at position 3 of the pyridine ring. (Free ligands are not depicted)

2.2. Py₂N₂ ligands.

The synthesis of 2,11-diaza[3,3](2,6)pyridinophane **Py₂N₂** was independently reported in 1988 by Lehn⁴⁶ and Pappalardo,⁴⁷ respectively. Ligands of this architecture were also early applied as MRI CA,^{36,48,49} and served to prepare isolable stable complexes of a variety of metals providing a valuable tool to study fundamental organometallic reaction mechanisms.^{50,51,52,53}

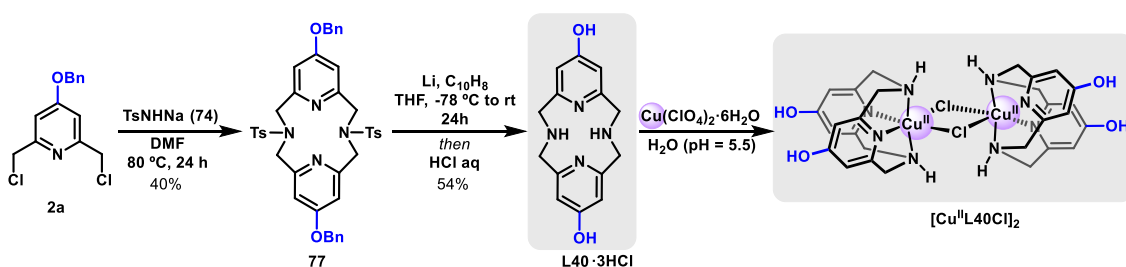
In spite of the importance of this class of ligands, the common synthesis is characterized by the need of tedious chromatography and extraction purifications due to the formation of 18-membered macrocycle trimer **75** as side product. In 2017, Mirica and co-workers reported an improved procedure for a faster and high yielding synthesis of **Py₂N₂**. The method notably simplified purification steps and enabled large scale synthesis to facilitate the availability of the ligand (Scheme 16).⁵⁴ The synthesis started with 2,6-pyridine dicarboxylic acid (**71**), which was converted into the corresponding methyl ester **72**. A successful reduction to diol **73** required a continuous extraction procedure using CHCl_3 to improve yield and separation from the reaction

mixture. Transformation of hydroxyl moieties into good leaving groups was performed by tosylation, which set the stage for the crucial dimerization in the presence of tosylamide monosodium salt **74**. At this stage, a clever method to separate the desired **76** from trimeric ligand **75** was based on the completely selective protonation of the former. Thus, **76**-HCl formed by the addition of a stoichiometric amount HCl (1.0 M) in EtOH (95% solution) was soluble while **75** is insoluble in these conditions. With this simple separation method, this step could be scaled-up to obtain 9.6 g (>16 mmol) of **76** with a remarkable high yield in a single batch. Finally, **Py₂N₂** was obtained after conventional tosyl deprotection. This route offers now a reliable access to large amounts of **Py₂N₂** as well as to (*non*)symmetric *N,N'*-dialkyl substituted ligands of this family.



Scheme 16. Practical and scalable synthesis of **Py₂N₂** ligand.

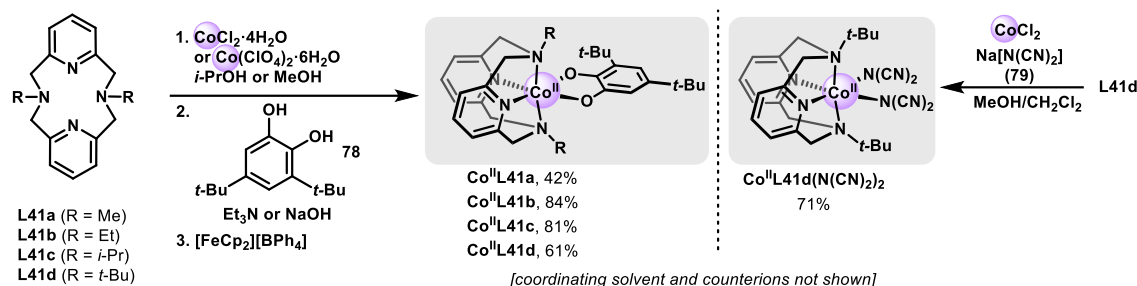
In line with its previous studies with OH-substituted pycen derivatives (see Scheme 2),^{10,11,12,13} Green's group also reported the synthesis of di-hydroxyl macrocyclic pyridinophane **L40**.⁵⁵ The ligand **L40** was prepared by dimerization of 4-benzyloxy-2,6-bis(chloromethyl)pyridine (**2a**) with tosyl amide **74** (Scheme 17). The removal of all protecting groups was performed in one step with lithium naphthalenide and acidic work-up. Ligand **L40** showed a better performance than the observed with pycen-OH analogues as antioxidant agent, keeping a high metabolic stability and low toxicity. Interestingly, when preparing the corresponding Cu(II) complex, the authors found that a dimeric complex **[Cu^{II}L40Cl]₂** with bridging chlorine atoms was formed. This is a rare example of isolated Cu(II) complex with **Py₂N₂**-type ligands.



Scheme 17. Synthesis of OH-disubstituted ligand **L40** and Cu(II) dimer complex **[Cu^{II}L40Cl]₂**.

With respect to metal complexes comprising **Py₂N₂**-type ligands, main attention has been devoted to the preparation of Co(II) complexes and the study of their electronic structures. Indeed, the group of Krüger,^{56,57} and Boskovic⁵⁸ reported the synthesis of various dioxolene-Co(II) complexes **Co^{II}L41** coordinated to *N,N'*-dialkyl substituted **Py₂N₂** ligands **L41** (Scheme 18). A related *cis*-dicyanamido Co(II) complex **Co^{II}L41d(N(CN)₂)₂** was also reported by Mondal and co-workers.⁵⁹ Importantly, these studies served to rationalize electronic properties of the Co(II)

complexes. Particularly spin cross-over transitions and valence tautomerism were described as function of the size of the alkyl groups of the ligand. This knowledge can be exploited for the design of ligands that might finely tune these properties and exploit them for instance in developing fast molecular switches.



Scheme 18. $\text{Co}^{\text{II}}\text{L41}$ complexes with N,N' -dialkyl-substituted Py_2N_2 -type ligands.

3. Reactivity of metal complexes coordinated to pyridine-containing 12-membered tetraazamacrocycles.

In spite of the strong focus of metal complexes formed with 12-membered macrocyclic pyridine-containing ligands in the medicine, the use in more conventional chemistry is notable. This section describes the rich reactivity of these complexes in stoichiometric reactions or their uses as catalysts.

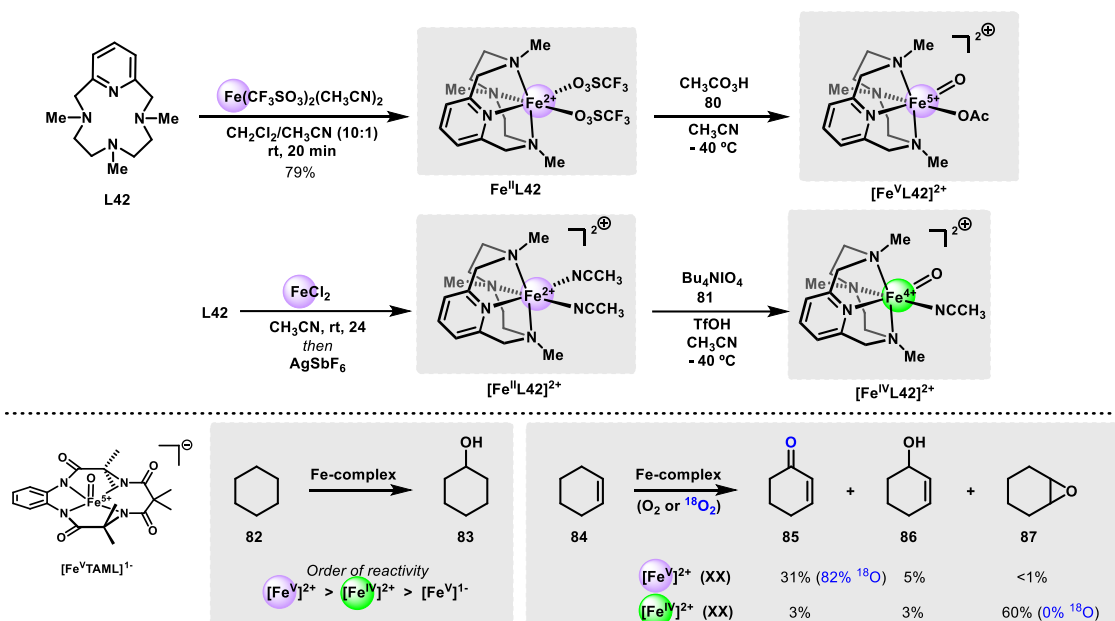
3.1. Iron-catalysed oxidation reactions.

Enzymes containing high valence iron complexes are the most frequent biomolecules to accomplish oxidation processes in living organisms.⁶⁰ In order to replicate this function out of the cell, simpler synthetic models based on non-heme oxoiron(IV) complexes for C–H bond oxidation,⁶¹ or oxoiron(IV) complexes mimicking Rieske oxygenase chemistry,⁶² are matter of exhaustive research.

In the context of these studies, the use of pyridine-containing tetraazamacrocyclic ligands proved to be fundamental due to their ability to stabilize high valence metal complex intermediates. With obvious interest in catalytic efficiency, this ability is proposed to be essential in the stabilization of the postulated highly oxidized intermediates. In this regard, collaborative efforts have resulted in the spectroscopic characterization with several techniques of non-heme iron(V) complexes bearing pycnen ligand derivatives (Scheme 19).^{63,64,65} In particular, ligand **L42** was used to prepare the corresponding iron(II) complex $\text{Fe}^{\text{II}}\text{L42}$. In the presence of peracetic acid (**80**), the complex was converted into a cationic oxoiron(V) species $[\text{Fe}^{\text{V}}\text{L42}]^{2+}$. Importantly, this species showed enough life time to be characterized by spectroscopic methods (EPR, Mossbauer, UV-Vis or Raman) and XAS analysis. As main features, species $[\text{Fe}^{\text{V}}\text{L42}]^{2+}$ presented a low spin state ($S = \frac{1}{2}$) oxoiron(V) center.

The catalytic performance of this compound was compared with previously reported TAML-iron(V) complex $[\text{Fe}^{\text{V}}\text{TAML}]^{1-}$,⁶⁶ in the oxidation reaction of cyclohexane (**82**) to cyclohexanol (**83**). Interestingly, iron complex $[\text{Fe}^{\text{V}}\text{L42}]^{2+}$ showed a 10^4 -fold faster reaction rate than the measured with TAML complex. This fact might be attributed to the neutral nature of pycnen ligands, which reduces iron(V) electrophilicity and, therefore, increases its oxidative ability.

Subsequent studies tackled the study of oxoiron(IV) species.⁶⁷ In this case, cationic iron(II) complex $[\text{Fe}^{\text{II}}\text{L42}]^{2+}$ was prepared. Subsequent treatment with tetrabutyl ammonium metaperiodate (**81**) and TfOH to generate oxoiron(IV) species $[\text{Fe}^{\text{IV}}\text{L42}]^{2+}$, which was spectroscopically characterized (UV-Vis, Mossbauer, Raman and XAS analysis). The electronic state of $[\text{Fe}^{\text{IV}}\text{L42}]^{2+}$ corresponds to a spin value $S = 1$ and geometry indicated a *trans* situation of the O-atom with respect to pyridine. Comparative studies indicated that iron(V) complexes are more reactive than those of iron(IV) in the oxidation of cyclohexene (**82**). Interestingly, oxidation of cyclohexene (**84**) with both complexes led to different reaction outcomes. While oxoiron(IV) complex preferentially yielded allylic oxidation to form **85** and **86**, oxoiron(V) complex afforded cyclohexene oxide (**87**) with high selectivity. Experiments using isotopically labelled $^{18}\text{O}_2$ gave valuable mechanistic information, which agrees with a direct O-atom transfer from oxoiron(V) complex to the alkene.⁶⁸



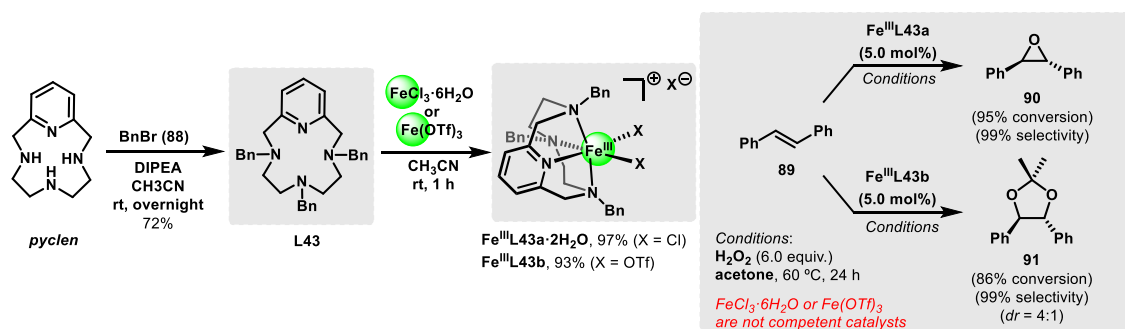
Scheme 19. Synthesis of well-characterized iron(IV/V) complexes with **L42** and their activities in oxidation reactions.

The ability to catalyze oxidation reactions using iron complexes decorated with pycen ligands was exploited by Caselli and co-workers. (Scheme 20).⁶⁹ In this study, the synthesis of pycen ligand **L43**, as well as the corresponding iron(III) chloride or triflate complexes $\text{Fe}^{\text{III}}\text{L43a-b}$ were described. Electronic characterization indicates that iron(III) chloride complex had a mixed spin state ($S=1/2$ and $S=5/2$), while iron(III) triflate showed single spin state $S=5/2$.

Noteworthy, a remarkable catalyst-controlled product selectivity was observed in the oxidation of alkenes using H_2O_2 as oxidant and acetone as solvent. Indeed, using *E*-stilbene (**89**), chloride complex $\text{Fe}^{\text{III}}\text{L43a}$ led selectively to the formation of the *E*-stilbene oxide (**90**), while triflate complex $\text{Fe}^{\text{III}}\text{L43b}$ afforded the protected diol **91**. The scope of both oxidations reactions was demonstrated with the use of highly substituted alkenes, aliphatic alkenes and limonene, which showed a complete preference for the oxidation in the internal alkene.

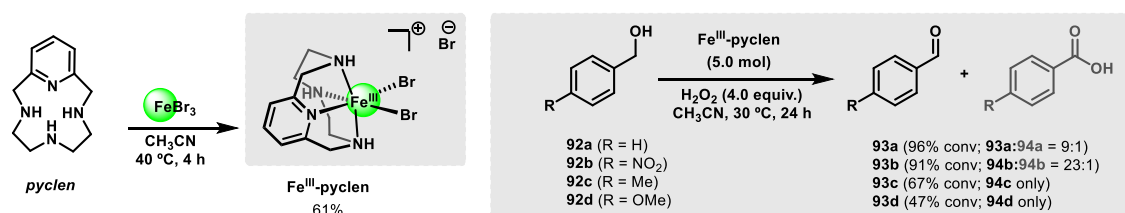
With respect to the mechanism, complex $\text{Fe}^{\text{III}}\text{L43a}$ should operate through a direct oxygen atom transfer to the alkene. On the contrary, the results observed with $\text{Fe}^{\text{III}}\text{L43b}$ catalysts involve a

more complicated mechanistic scenario. Although direct *syn*-hydroxylation followed by Lewis- or Brønsted acid-catalysed formation of **91** might be operative,⁷⁰ detailed control experiments point to a crucial role of unavoidable amounts of triflic acid, which might mediate the transformation of the epoxide into the protected diol.⁷¹ Regardless the catalyst employed, it is important to highlight the role of the pyridine-containing ligand, since the reaction with simple iron salts did not provide any oxidation product. Moreover, these iron(III) complexes worked well with a more appealing oxidant as H₂O₂ in contrast to iron(II) complexes that require peracids as the oxidant.



Scheme 20. Catalyst-controlled alkene oxidation using iron(III) complexes **Fe^{III}L43a-b**.

In line with the above mentioned work, highly selective alcohol oxidation reactions were reported by Caselli and co-workers (Scheme 21).⁷² In this case, a well-defined iron(III) bromide complex with *pyclen* proved a suitable catalyst for the oxidation of primary alcohols to aldehydes. In particular, benzyl alcohols **92a-d** could be converted into benzaldehydes **93a-d** with, in some cases, suppression of the carboxylic acid formation. Notably, the oxidation took place under mild reaction conditions using convenient H₂O₂ as oxidant. Regarding the scope, benzylic alcohols with weaker C–H BDE worked well, while aliphatic alcohols still constitute a challenge in this transformation. Although detailed mechanistic studies are still pending, hydroperoxoiron(III) species might be involved. In addition, radical-clock experiments indicated that $1e^-$ mechanism might compete with traditionally proposed $2e^-$ processes. Although simple iron(III) bromide was promoting the reaction, its performance was inferior both in terms of conversion and selectivity pointing out yet again to the relevance of the ligand.



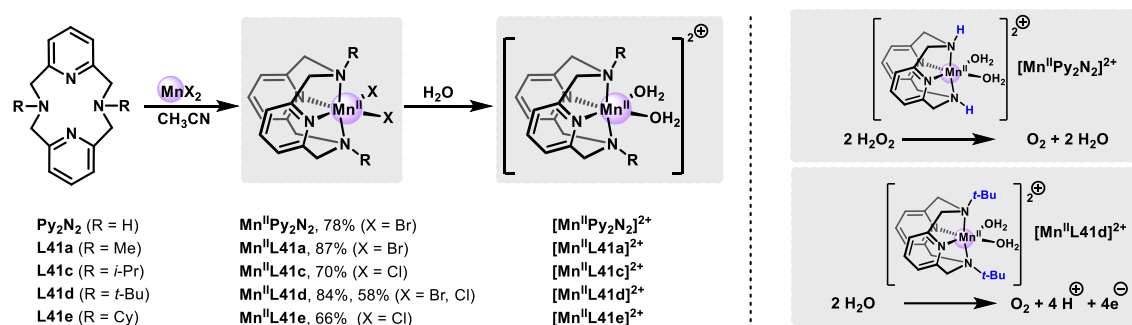
Scheme 21. Fe^{III}-*pyclen* complex in selective oxidations of alcohols to aldehydes.

3.2. Manganese-catalysed oxidation reactions.

The ubiquitous role played by manganese in biological chemistry,^{73,74} as exemplified by superoxide dismutase (Mn-SOD), manganese catalase (Mn-CAT) or the oxygen-evolving complex (OEC) within photosystem II (PSII), has triggered the research of a huge number of biomimetic manganese complexes. Again, 12-membered pyridine-containing tetraazamacrocycles such as

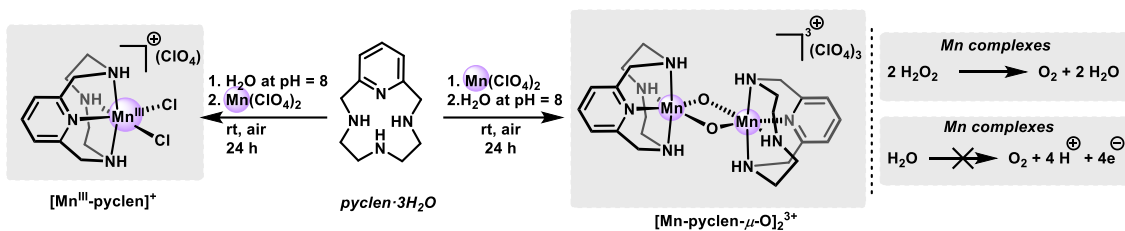
pyclen or **Py₂N₂** proved early their ability to allow access to Mn-high oxidation states as demonstrated experimentally and by DFT calculations described by Girerd and co-workers.⁷⁵

More recently, Smith and co-workers started a deep investigation regarding fine tuning of the properties of complexes bearing Py₂N₂ ligands with different steric requirements (Scheme 22).^{76,77,78} With respect to Mn(II) complexes, they prepared a series of cationic complexes **[Mn^{II}L41]²⁺** showing alkyl groups with different sizes and donor strengths. The substitution had a remarkable impact in the catalytic properties of the complexes. For instance, H₂O₂ disproportionation reaction (catalase activity) was promoted by **[Mn^{II}Py₂N₂]²⁺** complex (R = H), while bulkier substituents slowed down the reaction rates or completely inhibited the process, as observed with the bulkier complex **[Mn^{II}L41]²⁺** (R = *t*-Bu) of the series.^{78,79} Interestingly, the opposite reactivity trend was reported for the electrochemical oxidation of water to molecular oxygen. Indeed, **[Mn^{II}Py₂N₂]²⁺** complex was totally inactive in contrast to **[Mn^{II}L41]²⁺** complex, which showed the highest catalytic activity of the group. This fact was attributed to the increased size and donor strength of the pyridinophane ligand, which provided the required stability for Mn(III) or higher oxidation states postulated as intermediates.⁸⁰ Notably, the authors highlighted the critical role of the pyridinophane ligand. Thus, the ligand is responsible of a suitable geometric environment with good flexibility in promoting a range of different N–Mn–N bond angles, which finally favours the critical O–O bond formation.



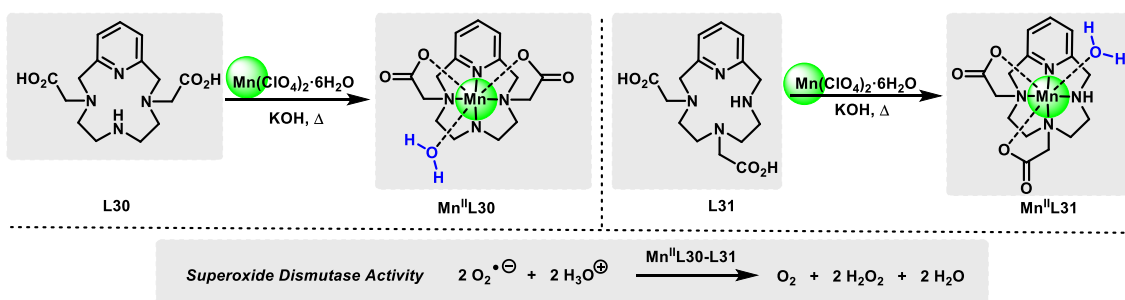
Scheme 22. Synthesis of Mn(II) complexes with Py₂N₂-type ligands and substitution-dependent oxidation reactions.

The catalase-like activity of Mn(II) complexes of pyclen macrocyclic ligands has also been object of a more recent study (Scheme 23).⁸¹ Monomeric and dimeric Mn complexes **Mn^{III}-pyclen** and **[Mn-pyclen-μ-O]₂** were prepared under aerobic selectively by choosing when the pH should be adjusted during the process. Pyridine ring in the ligand played a pivotal role in H₂O₂ disproportionation reactions. Thus, Mn(III) pyclen complexes showed better TON and TOF values than the corresponding pyridine-lacking 1,4,7,10-tetraazacyclododecane (**cyclen**) complex at 6–8 pH range. In contrast, TON/TOF values are smaller than the observed for Mn(II) complexes with Py₂N₂-type ligands. Noteworthy, experimental evidences for **Py₂N₂** complex **Mn^{II}-Py₂N₂**, clearly indicates a monomeric catalyst state during the oxygen evolution,^{76,77} while spectroscopic evidences points to the dimeric **[Mn^{III}-Mn^{IV}(μ-O)₂]³⁺** species with **Mn^{III}-pyclen**, which is likely the truly active catalyst. Unfortunately, **Mn^{III}-pyclen** were not capable of promoting water oxidation.



Scheme 23. Synthesis of mono- and dimeric Mn(II)-pyclen complexes in oxidation reactions.

Superoxide dismutase activity (SOD) studies of Mn(II) complexes **Mn^{II}L30** and **Mn^{II}L31** with two pyclen based ligands functionalized with acetate pendant arms has been reported (Scheme 24).³⁵ These complexes showed SOD activity, in contrast to the corresponding Mn(II)-PCTA complex. This fact was attributed to coordinative saturated structure typical of PCTA complexes, which makes them kinetically robust. In contrast, the presence of an inner sphere water molecule in complexes **Mn^{II}L30** and **Mn^{II}L31** made them reactive in SOD processes. Indeed, coordinated water dissociation allows the interaction of Mn(II) with the O₂⁻ radical anion, promoting its decomposition. Nevertheless, catalytic activities of both complexes is considerably more modest than those normally observed for others Mn(II)-SOD mimetic models.⁸²



Scheme 24. Synthesis of Mn^{II}L30 and Mn^{II}L31 with SOD activity.

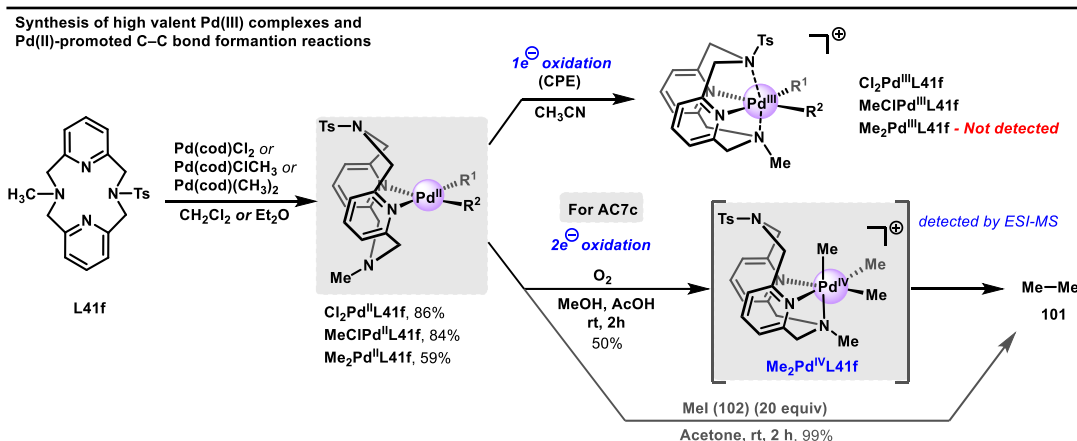
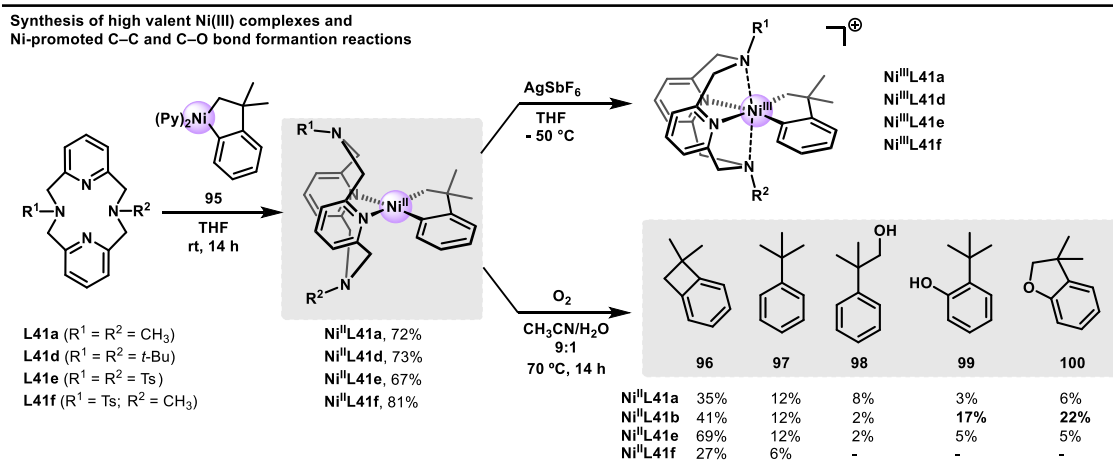
3.3. Nickel and palladium complexes in C–C or C–X oxidative couplings.

Nickel and palladium catalysts play a prominent role in C–C and C–heteroatom bond formation *via* cross coupling reactions.⁸³ It is generally assumed that group 10 metals operate in these reactions through low oxidation states (M(0), M(I) or M(II)). However, recent studies indicated that higher oxidation states of Ni can be conveniently applied in catalytic C–C and C–X bond formation reactions.^{84,85} In this regard, the capability of pyridine-containing tetraazamacrocyclic ligands to stabilize uncommon oxidation states has been thoroughly investigated by Mirica and co-workers in the last years. Thus, they have reported a number of Ni(III)/Ni(IV) pyridinophane complexes which were able to promote oxidative C–C and C–X bond formation reactions in stoichiometric processes.⁸⁶ Moreover, they also showed that isolable and fully characterized neutral and cationic Ni(III)-complexes coordinated to pyridinophane Py₂N₂ ligands were catalytically relevant in cross-coupling reactions.^{87,88}

More recently, the group of Prof. Mirica expanded the scope of the reactivity high valence nickel(III) complexes showing their ability to promote C–C and C–O bond formation reactions using O₂ or H₂O₂ as convenient oxidants (Scheme 25).⁸⁹ Square planar nickel(II)

complexes **Ni^{II}-L41** were simply prepared using Ni(II) cyclometallated species **95** and several Py₂N₂-type ligands. Those complexes underwent mild oxidation with AgSbF₆ enabling a straightforward access to high oxidation state nickel(III) complexes **Ni^{III}-L41**, which could be isolated and fully characterized. Interestingly, oxidation of nickel(II) complexes **Ni^{II}-L41** with most ideal oxidants (O₂ or H₂O₂) led to compounds **96-100** by means of C–C and C–O bond formation reactions, which likely occurred *via* nickel(IV) intermediates. The product distribution could be rationalized with the ligand properties. Thus, the presence of electron withdrawing *N*-Ts substituent favoured C–C bond forming reactions, since the reductive elimination occurs faster for five or four coordinated Ni complexes. On the contrary, non-symmetric ligand **L41f**, reacted preferentially via C–O bond formation. This fact was attributed to the supposed superior ability to stabilize high valence Ni(IV) intermediates, which might favour processes involving oxonickel(IV) species. Finally, the steric bulk in **L41d** ligand might prevent any exogenous reactivity suppressing C–O bond formation reactions as observed.

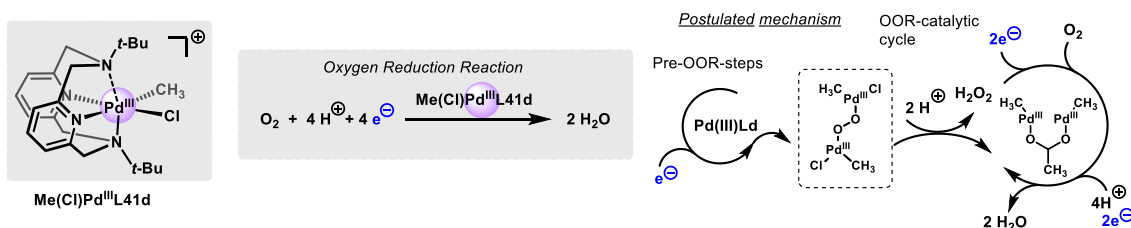
Mirica's group has also taken advantage of the properties of Py₂N₂ ligands to study oxidative C–C bond coupling in palladium complexes.⁹⁰ Remarkably, Pd(II) complexes were readily oxidised by means of O₂ or peroxides to form stable cationic Pd(III) intermediates, which easily undergo C–C bond coupling to form ethane (**101**) by reductive elimination. Very recently, they studied the reactivity of various pyridinophane Pd(II) complexes **Pd^{II}-L41f** derived from non-symmetric **L41f** (Scheme 25).⁹¹ The use of this ligand resulted in lower stabilities of high valence Pd(III) and Pd(IV) complexes with respect to previously reported examples with *N*-alkyl-substituted Py₂N₂. Nevertheless, the formation of pseudo-tridentate **Cl₂Pd^{III}L41f** and **Me(Cl)Pd^{III}L41f** complexes by 1e⁻ oxidation process was experimentally confirmed by EPR spectroscopy. In contrast, the characterization of the corresponding **Me₂Pd^{III}L41f** or **Me₂Pd^{IV}L41f** generated by 1e⁻ or 2e⁻ oxidation processes remained elusive. This translates into higher reactivity since fast formation of ethane (**101**) was observed under very mild reaction conditions. In this case, key **Me₂Pd^{IV}L41f** intermediate was detected by ESI-MS. Moreover, the fast reaction of complex **Me₂Pd^{III}L41f** with MeI (**102**) to give cleanly ethane provided additional evidence of an easy oxidative addition. It should be noticed that, even in the presence of a protic solvent and O₂, generation of methane or products arising via C–O bond formation were not detected.



Scheme 25. Synthesis of Ni and Pd complexes with Py₂N₂ ligands and their uses in C–C and C–O bond formation reactions.

3.4. Palladium and cobalt complexes in reduction reactions.

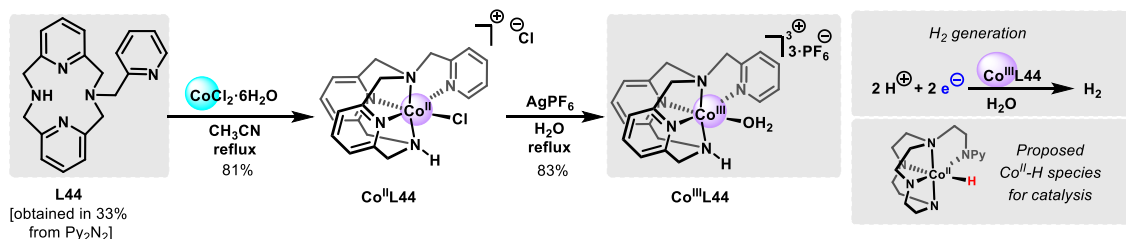
While the use of pyridine-containing tetraazamacrocycles as ligands in metal-catalysed oxidation reactions is common, the use of metal pyridinophane complexes in catalytic reduction reactions is very rare. In this sense, Mirica and Sinha recently reported the first electro-catalytic oxygen reduction reaction (ORR) to H₂O using a molecular palladium complex (Scheme 26).⁹² In this case, robust cationic Pd(III) complex **Me(Cl)Pd^{III}L41d**,⁹³ was capable of promoting the ORR under low potentials in the presence of moderate to weak acids such as AcOH. Interestingly, the ORR could be accomplished under homo- or heterogeneous conditions. While a deep knowledge of this transformation is still required, the first mechanistic studies suggested initial steps involving Pd(III) dimeric species, likely with a Pd-peroxo-Pd structure, followed by true ORR in which an acetate-bridge Pd(III) dimer might be relevant.



Scheme 26. Me(Cl)Pd^{III}L41d for electrocatalytic oxygen reduction reaction.

Another example of reduction reactions was reported by Webster, Zhao and co-workers describing the electro- or photocatalytic generation of H₂ from water with soluble Co(III) complex **Co^{III}L44** (Scheme 27).⁹⁴ The corresponding ligand **L44** was prepared from **Py₂N₂** through a controlled benzylation, subsequent treatment with CoCl₂ enabled the preparation of complex **Co^{II}L44**. Finally, oxidation with AgPF₆ in water led to the formation of the required Co(III) complex **Co^{III}L44**, with an inner-sphere water molecule. Unfortunately, this complex could not be characterized by X-Ray diffraction.

Observed TON-values of 140 and 200 (mol H₂/mol catalyst) for the electro- (pH = 7) or the photocatalytic production (pH = 6), respectively, were lower than those observed for related macrocyclic cobalt complexes.⁹⁵ Nevertheless, electrochemical studies showed that **L44** has a good electron-donating ability compared to linear ligands and that reduced species of **Co^{III}L44** are then less stabilized. Mechanistic studies suggested that a pentacoordinated Co(II)-H species is involved during H₂ generation providing a hydride. The most likely scenario is that external water delivers the proton. Although protonated ligand might also serve as proton source, computational studies indicated that this pathway is energetically disfavoured.

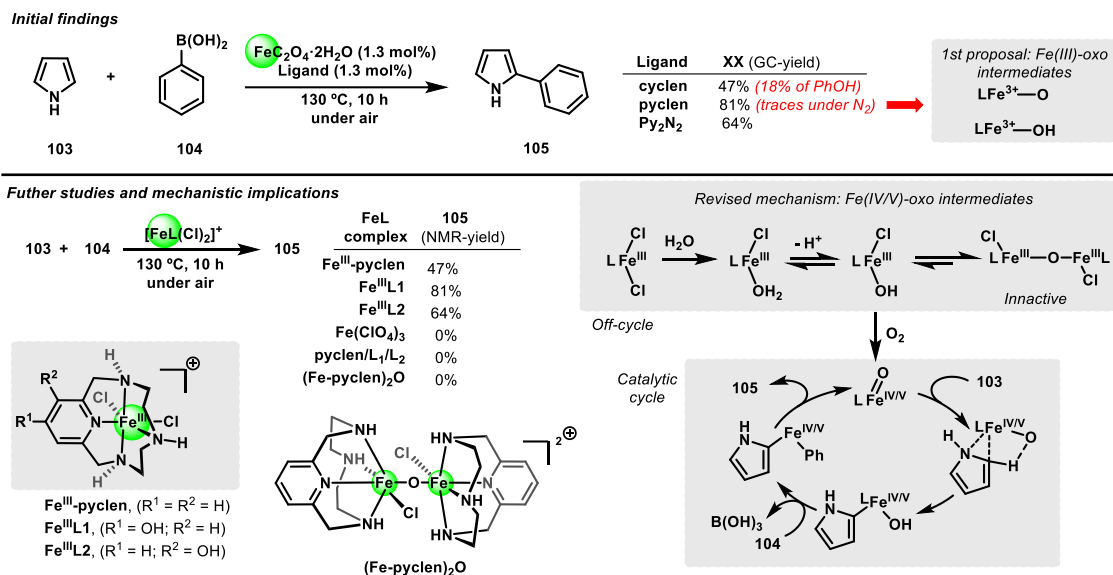


Scheme 27. Pentacoordinated **Co^{III}L44** complex for H₂ generation from water.

3.5. Iron-catalysed C–C bond formation through direct C–H functionalization.

The use of iron(II)-pyclen complexes as catalysts in cross-coupling chemistry, a field still plainly dominated by palladium and to a lesser extent by nickel, was reported by Wen and co-workers in 2010. Particularly, they showed that the simple catalytic system comprising iron(II) oxalate and **pyclen** or **Py₂N₂** as ligands were able to promote a direct C–H arylation with aryl boronic acids and pyrroles, which were used as solvent (Scheme 28).⁹⁶ The reaction proceeded regioselectively at position 2 of the pyrrole (**103**) with a reasonable broad scope and efficiency. Importantly, the authors noticed that oxygen was required for the reaction since under inert conditions the reaction failed. Accordingly, the participation of oxo-iron complex intermediates as truly catalytically active species were preliminarily postulated. Notably, the corresponding cyclen analogue gave rise to lower yields and appreciable amounts of phenol derived from **104**. This fact underlines again the ability of pyridine-containing macrocycles to stabilize highly oxidized intermediates. Later, the Prof. Green's group performed a more profound study of this coupling reaction (Scheme 28). First, they prepared a series of dichloro iron(III) pyclen complexes confirming the oxidation state of the metal, which showed a 5/2 spin state.⁹⁷ Cautious control experiments indicated that only complexes **Fe^{III}-pyclen**, **Fe^{III}L1** and **Fe^{III}L2** were catalytically active. Additional studies, including ligands lacking of pyridine ring, showed that iron(II/III) redox potential and *cis*-labile coordination sites were main factors for the success of the reaction.⁹⁸ The role of necessary oxygen was also studied and excluded oxidation of pyrrole and participation of radical intermediates.⁹⁹ Moreover, formation of bimetallic μ -oxo species, such

as **(Fe-pyclen)₂O**, was observed under the reaction conditions, yet independently prepared complex **(Fe-pyclen)₂O** was not able to promote the reactions. From this detailed studies, a more realistic proposal might involve the participation of Fe(IV)/(V)-oxo complex intermediates as responsible for the direct activation of the C–H bond of the pyrrole followed by transmetallation step and reductive elimination to yield the coupling product.



Scheme 28. Iron(III)-pyclen type complexes for C–C bond formation via C–H bond functionalization.

3.6. Copper-catalysed carbene transfer reactions.

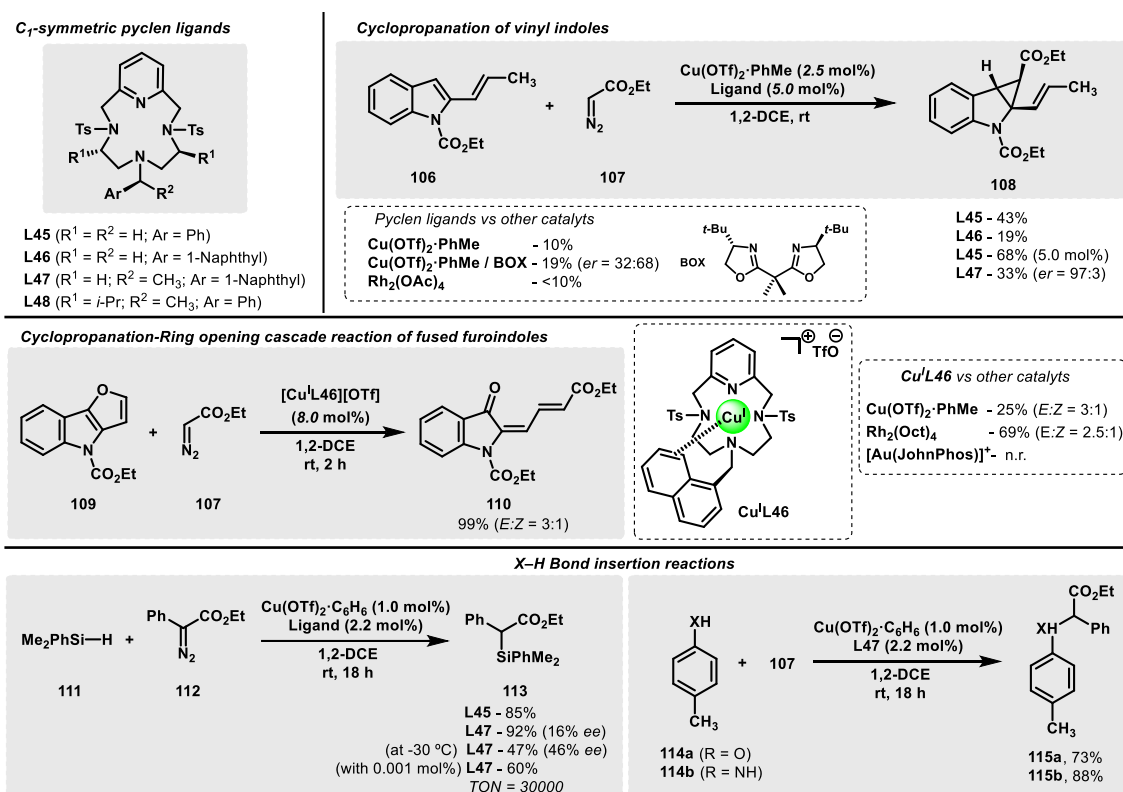
Caselli and co-workers have intensively studied the application of copper(I) complexes of 12-membered pyclen ligands in the asymmetric cyclopropanation of alkenes using diazo compounds as carbene precursors.^{100,101} In particular, C₁-symmetric pyclen derivative ligands **L45-L48**, which could be assembled in sequential manner to allow the functionalization of various positions (Scheme 29), have been employed in those studies. Interestingly, this reaction could be accomplished under flow conditions with CO₂ as carrier using a hydrogen bonding supported chiral copper(I)-**L48b** complex.¹⁰²

More recently, the ability of copper(I)-pyclen catalytic systems in cyclopropanation reactions was demonstrated. Specifically, the cyclopropanation of vinylindole derivatives with stabilized diazo compounds as the carbene source was reported by Pirovano and co-workers (Scheme 29).¹⁰³ Completely site- and diastereoselective cyclopropanation occurred at the indole ring, providing dearomatized vinylcyclopropanes, as illustrated for the reaction between 2-vinylindole **106** and diazo compound **107** to prepare cyclopropane derivative **108**, among other examples. Interestingly, the use of non-racemic chiral ligand **L47** enabled the asymmetric synthesis of **107** with a remarkable high enantioselectivity. The importance of the pyclen-type ligand deserves to be highlighted. Indeed, rhodium(II) or copper(I) catalysts, typically employed in cyclopropanation reactions, led to inferior results in terms of efficiency and also asymmetric induction, as compared with the use of famous BOX ligands.

In the same context, Brambilla and co-workers reported the reaction of 4*H*-furo[3,2-*b*]indoles with diazo compounds to provide conjugated oxoindolines, as indicated with the transformation

of fused furoindole **109** into indoline **110** by means of carbene transfer with diazo **107** (Scheme 29).¹⁰⁴ In this case, the use of well-defined copper(I) catalyst **Cu^IL46** led to better results than those obtained with *in-situ* generated catalyst. The overall transformation comprises a cyclopropanation/ring-opening reaction cascade. Once again, the ligand played a substantial role providing better results than the naked copper catalyst. In addition, rhodium or gold complexes used in closely related chemistry did not compete with **Cu^IL46**.

Apart from typical cyclopropanations, Vicente, Caselli and co-workers studied the X–H bond insertion reaction of carbenes generated from diazo compounds using pyclen-type ligands and copper (Scheme 29).¹⁰⁵ A catalytic system consisting of $\text{Cu}(\text{OTf})_2 \cdot \text{C}_6\text{H}_6$ and pyclen ligands **L45** or **L47** efficiently promoted the insertion of the carbenes derived from diazo compounds into Si–H bonds of a variety of hydrosilanes. For instance, the synthesis of functionalized silane **113** from diazo **112** and hydrosilane **111** could be accomplished even at low catalyst loadings with a remarkable high TON value. The use of **L47** provided moderate values of enantiomeric excess at low temperature in this transformation. Moreover, the same catalyst system proved capable of promoting O–H or N–H bond insertions in phenols or anilines in synthetically valuable yields.

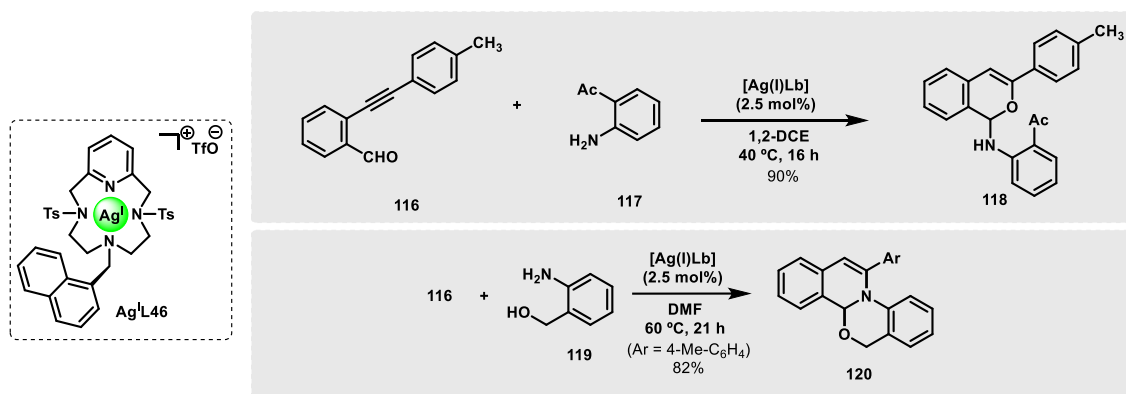


Scheme 29. Cu(I)-pyclen ligand complexes for carbene transfer reactions.

3.7. Silver-catalysed domino reactions involving cycloisomerizations.

Metal complex coordinated to pyclen-type ligands have been also employed in cycloisomerization reactions involving alkynes. Prior studies from Caselli, Abbiati and co-workers^{106,107,108} on this topic have been implemented recently. In 2020, they disclosed domino reactions of 2-alkynylbenzaldehyde derivatives with electron-poor anilines to prepare 1-aminoisochromene derivatives (Scheme 30).¹⁰⁹ The use of well-defined silver complex **Ag^IL46** enabled the synthesis of chromene **118** from aldehyde **116** and aniline **117**, as representative

example selected from the remarkable scope. Notably, naked silver salts led to poorer results. Next, a related domino reaction using the same aldehydes along with 2-(hydroxymethyl)anilines cleanly afforded benzoxazino isoquinoline derivatives, a biologically relevant polycyclic scaffold, in high yields (Scheme 30).¹¹⁰ The synthesis of compound **120** from aldehyde **116** and aniline **119** is shown herein as an illustrative example for a transformation which, again, showed a broad scope. In contrast, attempts to perform asymmetric transformations provided only modest results.



Scheme 30. Ag^IL46-catalyzed domino reactions of alkynylbenzaldehyde **116** with anilines.

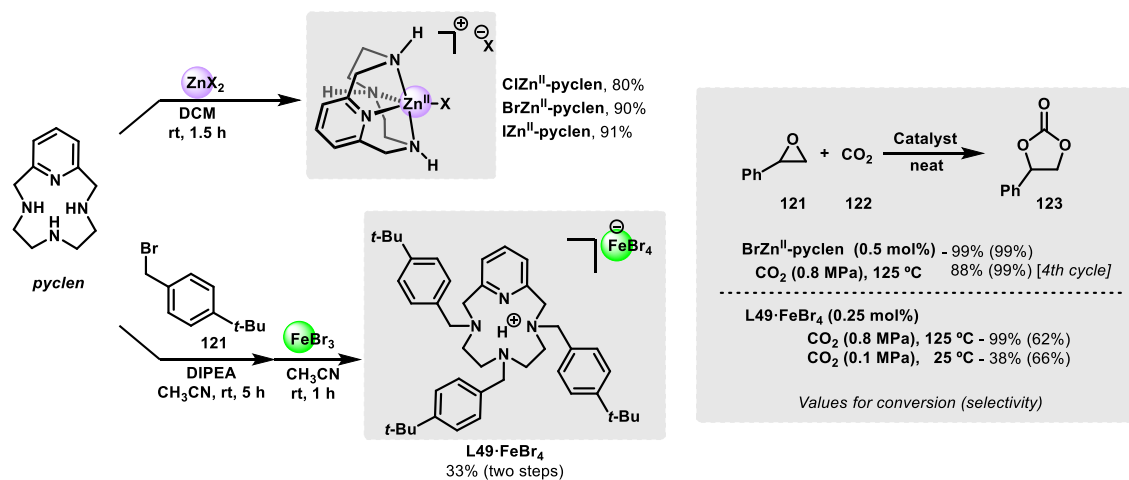
3.8. Zinc complexes and ferrates for the utilization of CO₂.

A mayor goal in current research is focused on developing methods to use pollutant CO₂ in the synthesis of high valued products. Among several alternatives, using CO₂ for the preparation of cyclic carbonates relies as one of the most interesting transformations. In this regard, Caselli and co-workers have recently disclosed that well-defined cationic Zn^{II}-pyclen complexes were a competent catalyst for utilization of CO₂ in cycloaddition reactions with terminal epoxides (Scheme 31).¹¹¹ In particular, zinc-pyclen complexes XZn^{II}-pyclen (X = Cl, Br, I) were easily prepared from zinc halide salts in very good yields and they could be fully characterized. X-Ray diffraction analysis of zinc cationic complexes revealed a distorted square pyramidal zinc environment, which provides a free coordination site on the zinc and might eventually make use of the outer-sphere anion.

These complexes showed a notable activity in the reaction of epoxides and CO₂ to yield cyclic carbonates, which could be efficiently obtained under solvent- and additive-free conditions at a moderate CO₂ pressure of 0.8 MPa. All zinc(II) complexes promoted the transformation, yet better results were obtained for the bromine complex BrZn^{II}-pyclen. The reaction worked nicely when accomplished with terminal epoxides, providing high yields and selectivities, as indicated for the formation of carbonate **123**. Moreover, the catalyst could be reused at least up-to four times, indicating its robustness. In contrast, limitations regarding challenging di- or trisubstituted epoxides are still to be addressed.

More recently, the same authors reported the preparation of new “ferrate” species L49·FeBr₄, obtained by reaction between FeBr₃ and a protonated pyclen ligand L49 (Scheme 31).¹¹² This species was also a competent stand-alone catalyst for the production of the cyclic carbonates from CO₂ and epoxides, which operated without the addition of any external nucleophile. L49·FeBr₄ proved to be active even under mild conditions (25 °C and 1 atm of CO₂) and a competent catalyst at higher temperatures, with reasonably good TOF values. In addition

to the fact that the iron is on the anion, protonated macrocyclic ligand was soluble due to the presence of bulky alkyl substituents on the nitrogen atoms.



Scheme 31. Synthesis of Zn(II) and ferrate pycen-derived complexes and its use for conversion of CO₂ into cyclic carbonates.

4. Outlook.

The chemistry of pyridine-containing 12-membered tetraazamacrocycles with **pycnen** or **Py₂N₂** skeleton is experiencing a remarkable growth in the recent years. In this review, we have provided an overview of newly prepared 12-membered pyridinophanes, in some cases showing a significant structural complexity. It should be noticed that these strategies, in spite of their apparent simplicity, are still challenging. Thus, rational designs in the synthesis on new ligands should definitely face issues related with green processes, atom and step economy, among others. This fact, along with the possibility to use less toxic metals might be further exploited in the development of more efficient and safe reagents for MRI and other applications in medicinal chemistry.

A number of studies indicated the relevance of the structure of the ligand, particularly of the pyridine ring. This can strongly influence the metal upon coordination and in some cases provide unique properties and reactivities. In redox chemistry, continuing studies on high oxidation states have allowed to shed light on the mechanisms of oxidative reactions catalysed by complexes mimicking enzymes, as well as the synthesis of extremely active catalysts for oxidation reactions. However, the stability of the ligand toward harsh oxidising conditions employed in catalysis still remains as a relevant challenge to address. Moreover, the applicability of this complex in reduction reactions remains underexplored and new findings are yet to come out.

The conformational flexibility and high coordination modularity displayed by these ligands represents an advantage to access different geometries of the metal centre facilitating changes in the oxidation state. In contrast, this property turns into a problem when attempting stereoselective reactions. In this sense, studies on stereoselective catalytic applications of pyridinophane ligands need to be tackled. We may anticipate an exciting future for this exceptional class ligands which should still find more applications in catalysis, especially if the current library and the possible modifications to these systems are soon further expanded.

5. Acknowledgements

We are particularly grateful to all our co-workers who have contributed to this research. Financial support from Ministerio de Economía y Competitividad, Agencia Estatal de Investigación (AEI), Fondo Europeo de Desarrollo Regional (FEDER) (Grants CTQ2016-76840-R and PID2019-107469RB), MUR-Italy (Ph.D. fellowships to N. P.) and the University of Milan (PSR 2020 – financed project “Catalytic strategies for the synthesis of high added-value molecules from bio-based starting materials”) is gratefully acknowledged.

6. References.

-
- ¹ K. M. Kadish, K. M. Smith and R. Guilard, *Handbook of Porphyrin Science*, World Scientific, Singapore, 2010
 - ² D. H. Busch, *Acc. Chem. Res.*, 2002, **11**, 392–400.
 - ³ P. Caravan, J. J. Ellison, T. J. McMurry and R. B. Lauffer, *Chem. Rev.*, 1999, **99**, 2293–2352.
 - ⁴ V. C. Pierre, M. J. Allen and P. Caravan, *JBIC J. Biol. Inorg. Chem.* 2014 **192**, 2014, **19**, 127–131.
 - ⁵ T. J. Clough, L. Jiang, K. L. Wong and N. J. Long, *Nat. Commun.* 2019 **101**, 2019, **10**, 1–14.
 - ⁶ J. Wahsner, E. M. Gale, A. Rodríguez-Rodríguez and P. Caravan, *Chem. Rev.*, 2018, **119**, 957–1057.
 - ⁷ G. Tseberlidis, D. Intriери and A. Caselli, *Eur. J. Inorg. Chem.*, 2017, **2017**, 3589–3603.
 - ⁸ J. E. Richman and T. J. Atkins, *J. Am. Chem. Soc.*, 1974, **96**, 2268–2270.
 - ⁹ K. M. Lincoln, T. E. Richardson, L. Rutter, P. Gonzalez, J. W. Simpkins and K. N. Green, *ACS Chem. Neurosci.*, 2012, **3**, 919–927.
 - ¹⁰ K. M. Lincoln, P. Gonzalez, T. E. Richardson, D. A. Julovich, R. Saunders, J. W. Simpkins and K. N. Green, *Chem. Commun.*, 2013, **49**, 2712–2714.
 - ¹¹ K. M. Lincoln, M. E. Offutt, T. D. Hayden, R. E. Saunders and K. N. Green, *Inorg. Chem.*, 2014, **53**, 1406–1416.
 - ¹² M. A. Mekhail, K. Pota, T. M. Schwartz and K. N. Green, *RSC Adv.*, 2020, **10**, 31165–31170.
 - ¹³ K. N. Green, K. Pota, G. Tircsó, R. A. Gogolák, O. Kinsinger, C. Davda, K. Blain, S. M. Brewer, P. Gonzalez, H. M. Johnston and G. Akkaraju, *Dalt. Trans.*, 2019, **48**, 12430–12439.
 - ¹⁴ A. Yepremyan, M. A. Mekhail, B. P. Niebuhr, K. Pota, N. Sadagopan, T. M. Schwartz and K. N. Green, *J. Org. Chem.*, 2020, **85**, 4988–4998.
 - ¹⁵ I. Pont, J. González-García, M. Inclán, M. Reynolds, E. Delgado-Pinar, M. T. Albelda, R. Vilar and E. García-España, *Chem. A Eur. J.*, 2018, **24**, 10850–10858.
 - ¹⁶ B. Verdejo, A. Ferrer, S. Blasco, C. E. Castillo, J. González, J. Latorre, M. A. Máñez, M. G. Basallote, C. Soriano and E. García-España, *Inorg. Chem.*, 2007, **46**, 5707–5719.
 - ¹⁷ S. Aime, M. Botta, S. G. Crich, G. B. Giovenzana, G. Jommi, R. Pagliarin and M. Sisti, *Inorg. Chem.*, 1997, **36**, 2992–3000.
 - ¹⁸ M. Enel, N. Leygue, N. Saffon, C. Galaup and C. Picard, *Eur. J. Org. Chem.*, 2018, **2018**, 1765–1773.
 - ¹⁹ C. Galaup, J. M. Couchet, S. Bedel, P. Tisnès and C. Picard, *J. Org. Chem.*, 2005, **70**, 2274–2284.
 - ²⁰ N. Leygue, M. Enel, A. Diallo, B. Mestre-Voegtli, C. Galaup and C. Picard, *Eur. J. Org. Chem.*, 2019, **2019**, 2899–2913.
 - ²¹ (a) M. Le Fur, R. Tripier, O. Rousseaux, M. Beyler, France Patent FR3046172 A1, 2017. (b) M. Le Fur, R. Tripier, O. Rousseaux, M. Beyler, World Intellectual Property Organization, WO2017109217 A1, 2017.
 - ²² M. Le Fur, M. Beyler, E. Molnár, O. Fougère, D. Esteban-Gómez, G. Tircsó, C. Platas-Iglesias, N. Lepareur, O. Rousseaux and R. Tripier, *Chem. Commun.*, 2017, **53**, 9534–9537.
 - ²³ M. Le Fur, M. Beyler, E. Molnár, O. Fougère, D. Esteban-Gómez, G. Tircsó, C. Platas-Iglesias, N. Lepareur, O. Rousseaux and R. Tripier, *Inorg. Chem.*, 2018, **57**, 2051–2063.
 - ²⁴ G. Nizou, C. Favaretto, F. Borgna, P. V. Grundler, N. Saffon-Merceron, C. Platas-Iglesias, O. Fougère, O. Rousseaux, N. P. Van Der Meulen, C. Müller, M. Beyler and R. Tripier, *Inorg. Chem.*, 2020, **59**, 11736–11748.
 - ²⁵ M. Le Fur, E. Molnár, M. Beyler, O. Fougère, D. Esteban-Gómez, O. Rousseaux, R. Tripier, G. Tircsó and C. Platas-Iglesias, *Inorg. Chem.*, 2018, **57**, 6932–6945.

- ²⁶ G. Nizou, E. Molnár, N. Hamon, F. K. Kálmán, O. Fougère, O. Rousseaux, D. Esteban-Gómez, C. Platas-Iglesias, M. Beyler, G. Tircsó and R. Tripier, *Inorg. Chem.*, 2021, **60**, 2390–2405.
- ²⁷ N. Hamon, M. Galland, M. Le Fur, A. Roux, A. Duperray, A. Grichine, C. Andraud, B. Le Guennic, M. Beyler, O. Maury and R. Tripier, *Chem. Commun.*, 2018, **54**, 6173–6176.
- ²⁸ N. Hamon, A. Roux, M. Beyler, J. C. Mulatier, C. Andraud, C. Nguyen, M. Maynadier, N. Bettache, A. Duperray, A. Grichine, S. Brasselet, M. Gary-Bobo, O. Maury and R. Tripier, *J. Am. Chem. Soc.*, 2020, **142**, 10184–10197.
- ²⁹ M. Le Fur, O. Fougère, N. Lepareur, O. Rousseaux, R. Tripier and M. Beyler, *Metallomics*, 2021, **13**, 70.
- ³⁰ L. Abad Galán, N. Hamon, C. Nguyen, E. Molnár, J. Kiss, J. Mendy, K. Hadj-Kaddour, M. Onofre, G. Trencsényi, C. Monnereau, M. Beyler, G. Tircsó, M. Gary-Bobo, O. Maury and R. Tripier, *Inorg. Chem. Front.*, 2021, **8**, 2213–2224.
- ³¹ J. C. Friás, J. Soriano, S. Blasco, E. García-Espanã, A. Rodríguez-Rodríguez, D. Esteban-Gómez, F. Carniato, M. Botta, C. Platas-Iglesias and M. T. Albelda, *Inorg. Chem.*, 2020, **59**, 7306–7317.
- ³² L. Leone, L. Guarnieri, J. Martinelli, M. Sisti, A. Penoni, M. Botta and L. Tei, *Chem. Eur. J.*, 2021, **27**, 11811–11817.
- ³³ M. Devreux, C. Henoumont, F. Dioury, D. Stanicki, S. Boutry, L. Larbanoix, C. Ferroud, R. N. Muller and S. Laurent, *Eur. J. Inorg. Chem.*, 2019, **2019**, 3354–3365.
- ³⁴ Z. Garda, E. Molnár, F. K. Kálmán, R. Botár, V. Nagy, Z. Baranyai, E. Brücher, Z. Kovács, I. Tóth and G. Tircsó, *Front. Chem.*, 2018, **6**, 232.
- ³⁵ Z. Garda, E. Molnár, N. Hamon, J. L. Barriada, D. Esteban-Gómez, B. Váradi, V. Nagy, K. Pota, F. K. Kálmán, I. Tóth, N. Lihi, C. Platas-Iglesias, É. Tóth, R. Tripier and G. Tircsó, *Inorg. Chem.*, 2021, **60**, 1133–1148.
- ³⁶ W. D. Kim, D. C. Hrcir, G. E. Kiefer and A. Dean Sherry, *Inorg. Chem.*, 1995, **34**, 2225–2232.
- ³⁷ P. Pérez-Lourido, E. Madarasi, F. Antal, D. Esteban-Gómez, G. Wang, G. Angelovski, C. Platas-Iglesias, G. Tircsó and L. Valencia, *Dalt. Trans.*, 2022, **51**, 1580–1593.
- ³⁸ R. Botár, E. Molnár, G. Trencsényi, J. Kiss, F. K. Kálmán and G. Tircsó, *J. Am. Chem. Soc.*, 2020, **142**, 1662–1666.
- ³⁹ K. M. DiVittorio, F. T. Hofmann, J. R. Johnson, L. Abu-Esba and B. D. Smith, *Bioorg. Med. Chem.*, 2009, **17**, 141–148.
- ⁴⁰ F. K. Kálmán, F. K. Kálmán, V. Nagy, B. Váradi, Z. Garda, E. Molnár, G. Trencsényi, J. Kiss, S. Mème, W. Mème, É. Tóth and G. Tircsó, *J. Med. Chem.*, 2020, **63**, 6057–6065.
- ⁴¹ R. Botár, E. Molnár, Z. Garda, E. Madarasi, G. Trencsényi, J. Kiss, F. K. Kálmán and G. Tircsó, *Inorg. Chem. Front.*, 2022, **9**, 577–583.
- ⁴² T. Csupász, D. Szücs, F. K. Kálmán, O. Hollóczki, A. Fekete, D. Szikra, É. Tóth, I. Tóth and G. Tircsó, *Molecules*, 2022, **27**, 371.
- ⁴³ H. Su, C. Wu, J. Zhu, T. Miao, D. Wang, C. Xia, X. Zhao, Q. Gong, B. Song and H. Ai, *Dalt. Trans.*, 2012, **41**, 14480–14483.
- ⁴⁴ M. Devreux, C. Henoumont, F. Dioury, S. Boutry, O. Vacher, L. Vander Elst, M. Port, R. N. Muller, O. Sandre and S. Laurent, *Inorg. Chem.*, 2021, **60**, 3604–3619.
- ⁴⁵ M. G. Kim, S. H. Yoo, W. S. Chei, T. Y. Lee, H. M. Kim and J. Suh, *J. Biol. Inorg. Chem.*, 2010, **15**, 1023–1031.
- ⁴⁶ B. Alpha, E. Anklam, R. Deschenaux, J. -M Lehn and M. Pietraskiewicz, *Helv. Chim. Acta*, 1988, **71**, 1042–1052.
- ⁴⁷ F. Bottino, M. Di Grazia, S. Pappalardo, P. Finocchiaro, A. Mamo and F. R. Fronczek, *J. Org. Chem.*, 1988, **53**, 3521–3529.
- ⁴⁸ W. D. Kim, G. E. Kiefer, F. Maton, K. McMillan, R. N. Muller and A. Dean Sherry, *Inorg. Chem.*, 1995, **34**, 2233–2243.
- ⁴⁹ A. Roca-Sabio, C. S. Bonnet, M. Mato-Iglesias, D. Esteban-Gómez, É. Tóth, A. De Blas, T. Rodríguez-Blas and C. Platas-Iglesias, *Inorg. Chem.*, 2012, **51**, 10893–10903.
- ⁵⁰ W.-T. Lee, S. B. Muçoz, D. A. Dickie, J. M. Smith, W.-T. Lee, S. B. Muçoz, M. Smith and D. A. Dickie, *Angew. Chemie Int. Ed.*, 2014, **53**, 9856–9859.
- ⁵¹ B. Zheng, F. Tang, J. Luo, J. W. Schultz, N. P. Rath and L. M. Mirica, *J. Am. Chem. Soc.*, 2014, **136**, 6499–6504.
- ⁵² W. P. To, T. Wai-Shan Chow, C. W. Tse, X. Guan, J. S. Huang and C. M. Che, *Chem. Sci.*, 2015, **6**, 5891–5903.
- ⁵³ J. W. Schultz, K. Fuchigami, B. Zheng, N. P. Rath and L. M. Mirica, *J. Am. Chem. Soc.*, 2016, **138**, 12928–12934.
- ⁵⁴ A. J. Wessel, J. W. Schultz, F. Tang, H. Duan and L. M. Mirica, *Org. Biomol. Chem.*, 2017, **15**, 9923–9931.

- ⁵⁵ H. M. Johnston, K. Pota, M. M. Barnett, O. Kinsinger, P. Braden, T. M. Schwartz, E. Hoffer, N. Sadagopan, N. Nguyen, Y. Yu, P. Gonzalez, G. Tircsó, H. Wu, G. Akkaraju, M. J. Chumley and K. N. Green, *Inorg. Chem.*, 2019, **58**, 16771–16784.
- ⁵⁶ M. Graf, G. Wolmershäuser, H. Keim, S. Demeschko, F. Meyer and H. J. Krüger, *Angew. Chemie Int. Ed.*, 2010, **49**, 950–953.
- ⁵⁷ F. Rupp, K. Chevalier, M. Graf, M. Schmitz, H. Kelm, A. Grün, M. Zimmer, M. Gerhards, C. van Wüllen, H.-J. Krüger and R. Diller, *Chem. A Eur. J.*, 2017, **23**, 2119–2132.
- ⁵⁸ T. Tezgerevska, E. Rousset, R. W. Gable, G. N. L. Jameson, E. C. Sañudo, A. Starikova and C. Boskovic, *Dalt. Trans.*, 2019, **48**, 11674–11689.
- ⁵⁹ S. Ghosh, S. Selvamani, S. Mehta and A. Mondal, *Dalt. Trans.*, 2020, **49**, 9208–9212.
- ⁶⁰ S. Sahu and D. P. Goldberg, *J. Am. Chem. Soc.*, 2016, **138**, 11410–11428.
- ⁶¹ W. Nam, *Acc. Chem. Res.*, 2015, **48**, 2415–2423.
- ⁶² S. M. Barry and G. L. Challis, *ACS Catal.*, 2013, **3**, 2362–2370.
- ⁶³ J. Serrano-Plana, W. N. Oloo, L. Acosta-Rueda, K. K. Meier, B. Verdejo, E. García-España, M. G. Basallote, E. Münck, L. Que, A. Company and M. Costas, *J. Am. Chem. Soc.*, 2015, **137**, 15833–15842.
- ⁶⁴ W. N. Oloo, R. Banerjee, J. D. Lipscomb and L. Que, *J. Am. Chem. Soc.*, 2017, **139**, 17313–17326.
- ⁶⁵ R. Fan, J. Serrano-Plana, W. N. Oloo, A. Draksharapu, E. Delgado-Pinar, A. Company, V. Martin-Diaconescu, M. Borrell, J. Lloret-Fillol, E. García-España, Y. Guo, E. L. Bominaar, L. Que, M. Costas and E. Münck, *J. Am. Chem. Soc.*, 2018, **140**, 3916–3928.
- ⁶⁶ T. J. Collins and A. D. Ryabov, *Chem. Rev.*, 2017, **117**, 9140–9162.
- ⁶⁷ V. Dantignana, J. Serrano-Plana, A. Draksharapu, C. Magallón, S. Banerjee, R. Fan, I. Gamba, Y. Guo, L. Que, M. Costas and A. Company, *J. Am. Chem. Soc.*, 2019, **141**, 15078–15091.
- ⁶⁸ For additional information regarding the mechanisms, see Ref. 58 and Ref. 60.
- ⁶⁹ G. Tseberlidis, L. Demonti, V. Pirovano, M. Scavini, S. Cappelli, S. Rizzato, R. Vicente and A. Caselli, *ChemCatChem*, 2019, **11**, 4907–4915.
- ⁷⁰ A. Solladié-Cavallo, E. Choucair, M. Balaz, P. Lupattelli, C. Bonini and N. Di Blasio, *European J. Org. Chem.*, 2006, 3007–3011.
- ⁷¹ T. T. Dang, F. Boeck and L. Hintermann, *J. Org. Chem.*, 2011, **76**, 9353–9361.
- ⁷² N. Panza, A. di Biase, S. Rizzato, E. Gallo, G. Tseberlidis and A. Caselli, *European J. Org. Chem.*, 2020, **2020**, 6635–6644.
- ⁷³ S. J. Smith, K. S. Hadler, G. Schenk, G. R. Hanson and N. Mitić, *Manganese Metalloproteins in Metal in Biology* (Ed. G. Hanson and L. Berliner), Springer (New York), 2010, 273–341.
- ⁷⁴ S. J. Lippard, J. M. Berg, W. Zhu and N. G. J. Richards, *Essays Biochem.*, 2017, **61**, 259–270.
- ⁷⁵
- ⁷⁶
- ⁷⁷
- ⁷⁸ S. Xu, L. Bucinsky, M. Breza, J. Krzystek, C. H. Chen, M. Pink, J. Telsler and J. M. Smith, *Inorg. Chem.*, 2017, **56**, 14315–14325.
- ⁷⁹ Y. Y. Li, K. Ye, P. E. M. Siegbahn and R. Z. Liao, *ChemSusChem*, 2017, **10**, 903–911.
- ⁸⁰ D. W. Crandell, S. Xu, J. M. Smith and M. H. Baik, *Inorg. Chem.*, 2017, **56**, 4435–4445.
- ⁸¹ D. M. Freire, D. Beerli, K. Pota, H. M. Johnston, P. Palacios, B. S. Pierce, B. D. Sherman and K. N. Green, *Inorg. Chem. Front.*, 2020, **7**, 1573–1582.
- ⁸² R. Bonetta, *Chem. - A Eur. J.*, 2018, **24**, 5032–5041.
- ⁸³ A. de Meijere and F. Diederich, *Metal-Catalyzed Cross-Coupling Reactions*, Wiley VCH, Weinheim, New York, 2004.
- ⁸⁴ N. Nebra, *Molecules*, 2020, **25**, 1141.
- ⁸⁵ J. Shin, S. Gwon, S. Kim, J. Lee and K. Park, *J. Am. Chem. Soc.*, 2020, **142**, 4173–4183.
- ⁸⁶ Selected examples: (a) W. Zhou, J. W. Schultz, N. P. Rath and L. M. Mirica, *J. Am. Chem. Soc.*, 2015, **137**, 7604–7607. (b) W. Zhou, S. Zheng, J. W. Schultz, N. P. Rath and L. M. Mirica, *J. Am. Chem. Soc.*, 2016, **138**, 5777–5780. (c) W. Zhou, N. P. Rath and L. M. Mirica, *Dalt. Trans.*, 2016, **45**, 8693–8695.
- ⁸⁷ B. Zheng, F. Tang, J. Luo, J. W. Schultz, N. P. Rath and L. M. Mirica, *J. Am. Chem. Soc.*, 2014, **136**, 6499–6504.
- ⁸⁸ J. W. Schultz, K. Fuchigami, B. Zheng, N. P. Rath and L. M. Mirica, *J. Am. Chem. Soc.*, 2016, **138**, 12928–12934
- ⁸⁹ S. M. Smith, O. Planas, L. Gómez, N. P. Rath, X. Ribas and L. M. Mirica, *Chem. Sci.*, 2019, **10**, 10366–10372.

-
- ⁹⁰ Selected examples: (a) J. R. Khusnutdinova, N. P. Rath and L. M. Mirica, *J. Am. Chem. Soc.*, 2010, **132**, 7303–7305. (b) F. Tang, F. Qu, J. R. Khusnutdinova, N. P. Rath and L. M. Mirica, *Dalt. Trans.*, 2012, **41**, 14046–14050. (c) J. R. Khusnutdinova, N. P. Rath and L. M. Mirica, *J. Am. Chem. Soc.*, 2012, **134**, 2414–2422.
- ⁹¹ J. W. Schultz, N. P. Rath and L. M. Mirica, *Inorg. Chem.*, 2020, **59**, 11782–11792.
- ⁹² S. Sinha and L. M. Mirica, *ACS Catal.*, 2021, **11**, 5202–5211.
- ⁹³ J. R. Khusnutdinova, N. P. Rath and L. M. Mirica, *J. Am. Chem. Soc.*, 2010, **132**, 7303–7305.
- ⁹⁴ P. Wang, G. Liang, C. L. Boyd, C. E. Webster and X. Zhao, *Eur. J. Inorg. Chem.*, 2019, **2019**, 2134–2139.
- ⁹⁵ D. Basu, S. Mazumder, X. Shi, H. Baydoun, J. Niklas, O. Poluektov, H. B. Schlegel and C. N. Verani, *Angew. Chem. Int. Ed.* 2015, **54**, 2105–2110.
- ⁹⁶ J. Wen, S. Qin, L. F. Ma, L. Dong, J. Zhang, S. S. Liu, Y. S. Duan, S. Y. Chen, C. W. Hu and X. Q. Yu, *Org. Lett.*, 2010, **12**, 2694–2697.
- ⁹⁷ S. M. Brewer, P. M. Palacios, H. M. Johnston, B. S. Pierce and K. N. Green, *Inorg. Chim. Acta*, 2018, **478**, 139–147.
- ⁹⁸ S. M. Brewer, K. R. Wilson, D. G. Jones, E. W. Reinheimer, S. J. Archibald, T. J. Prior, M. A. Ayala, A. L. Foster, T. J. Hubin and K. N. Green, *Inorg. Chem.*, 2018, **57**, 8890–8902.
- ⁹⁹ S. M. Brewer, T. M. Schwartz, M. A. Mekhail, L. S. Turan, T. J. Prior, T. J. Hubin, B. G. Janesko and K. N. Green, *Organometallics*, 2021, **40**, 2467–2477.
- ¹⁰⁰ A. Caselli, F. Cesana, E. Gallo, N. Casati, P. MacChi, M. Sisti, G. Celentano and S. Cenini, *Dalt. Trans.*, 2008, 4202–4205.
- ¹⁰¹ B. Castano, S. Guidone, E. Gallo, F. Ragaini, N. Casati, P. MacChi, M. Sisti and A. Caselli, *Dalt. Trans.*, 2013, **42**, 2451–2462.
- ¹⁰² B. Castano, E. Gallo, D. J. Cole-Hamilton, V. Dal Santo, R. Psaro and A. Caselli, *Green Chem.*, 2014, **16**, 3202–3209.
- ¹⁰³ V. Pirovano, E. Brambilla and G. Tseberlidis, *Org. Lett.*, 2018, **20**, 405–408.
- ¹⁰⁴ V. Pirovano, A. Caselli, A. Colombo, C. Dragonetti, M. Giannangeli, E. Rossi and E. Brambilla, *ChemCatChem*, 2020, **12**, 5250–5255.
- ¹⁰⁵ G. Tseberlidis, A. Caselli and R. Vicente, *J. Organomet. Chem.*, 2017, **835**, 1–5.
- ¹⁰⁶ M. Dellacqua, B. Castano, C. Cecchini, T. Pedrazzini, V. Pirovano, E. Rossi, A. Caselli and G. Abbiati, *J. Org. Chem.*, 2014, **79**, 3494–3505.
- ¹⁰⁷ M. Trose, M. Dell'Acqua, T. Pedrazzini, V. Pirovano, E. Gallo, E. Rossi, A. Caselli and G. Abbiati, *J. Org. Chem.*, 2014, **79**, 7311–7320.
- ¹⁰⁸ G. Tseberlidis, M. Dell'Acqua, D. Valcarengi, E. Gallo, E. Rossi, G. Abbiati and A. Caselli, *RSC Adv.*, 2016, **6**, 97404–97419.
- ¹⁰⁹ V. Pirovano, G. Hamdan, D. Garanzini, E. Brambilla, E. Rossi, A. Caselli and G. Abbiati, *Eur. J. Org. Chem.*, 2020, **2020**, 2592–2599.
- ¹¹⁰ D. Garanzini, V. Pirovano, I. Menghi, G. Celentano, S. Rizzato, E. Rossi, A. Caselli and G. Abbiati, *Eur. J. Org. Chem.*, 2020, **2020**, 3660–3670.
- ¹¹¹ M. Cavalleri, N. Panza, A. Biase, G. Tseberlidis, S. Rizzato, G. Abbiati and A. Caselli, *European J. Org. Chem.*, 2021, **2021**, 2764–2771.
- ¹¹² N. Panza, A. Biase, E. Gallo and A. Caselli, *J. CO₂ Util.*, 2021, **51**, 101635.